Turun yliopisto
University of Turku

MICROTUBULE-MEDIATED PROTEIN TRANSPORT MECHANISMS DURING SPERMIOGENESIS

Mari Lehti

TURUN YLIOPISTON JULKAISUJA – ANNALES UNIVERSITATIS TURKUENSIS
Sarja - ser. D osa - tom. 1262 | Medica - Odontologica | Turku 2016

University of Turku

Faculty of Medicine
Institute of Biomedicine
Department of Physiology
Turku Doctoral Programme of Molecular Medicine (TuDMM)
Natural Resources Institute Finland (Luke)
Green technology
Genetic research

Supervised by

Docent Anu Sironen
Natural Resources Institute Finland (Luke)
Green technology
Genetic research
Jokioinen, Finland

Associate professor Noora Kotaja
Department of Physiology
Institute of Biomedicine
Faculty of Medicine
University of Turku
Turku, Finland

Reviewed by

Research Director Eleanor Coffey
Åbo Akademi University and
Turku Centre of Biotechnology
Turku, Finland

Professor Seppo Vainio
Laboratory of Developmental Biology
Biocenter Oulu
Faculty of Biochemistry and Molecular Medicine
Oulu Center for Cell-Matrix Research
University of Oulu
Oulu, Finland

Opponent

Professor Moira O'Bryan
Monash Biomedicine Discovery Institute
Department of Anatomy and Developmental Biology
Monash University
Clayton VIC 3800, Australia

Cover photo by Mari Lehti

The originality of this thesis has been checked in accordance with the University of Turku quality assurance system using the Turnitin OriginalityCheck service.

ISBN 978-951-29-6656-1 (PRINT)
ISBN 978-951-29-6657-8 (PDF)
ISSN 0355-9483 (Print)
ISSN 2343-3213 (Online)
Painosalama Oy - Turku, Finland 2016

To my family

ABSTRACT

Mari Lehti
Microtubule-mediated protein transport mechanisms during spermiogenesis

University of Turku, Faculty of Medicine, Institute of Biomedicine, Department of Physiology, Turku Doctoral Programme of Molecular Medicine (TuDMM), Natural Resources Institute Finland (Luke), Green technology

Annales Universitatis Turkuensis, Medica-Odontologica, Turku, 2016

Formation of cilia and flagella is a tightly controlled process organized by intraflagellar transport (IFT), for which two motor proteins, kinesin-2 and dynein, are responsible. The exact functions of IFT and IFT-related proteins in spermiogenesis are poorly understood in mammalian species. To investigate mechanisms of IFT during mouse spermatogenesis, a male germ cell-specific knockout mouse model for kinesin-2 subunit kinesin-like protein 3A (KIF3A) was generated. Depletion of KIF3A caused defects in sperm tail development and the core structure, the axoneme, failed to form. A transient microtubular platform, the manchette, surrounds the sperm head during spermiogenesis. In KIF3A-depleted mice, the manchette appeared constricted and its clearance was delayed, causing abnormal head shape, suggesting that IFT and KIF3A function are also important for manchette function. In addition, we identified the KIF1-binding protein (KBP) and the meiosis-specific nuclear structural protein 1 (MNS1) as a novel interaction candidates for KIF3A.

Sperm flagellar protein 2 (SPEF2) has been shown to localize in elongating spermatids, and its interaction with IFT-related protein IFT20 has been established. To characterize the function of SPEF2 in sperm tail formation, a male germ cell-specific conditional knockout mouse model for SPEF2 was generated (*Spef2* cKO). Depletion of SPEF2 caused defects in axoneme formation, and similar defects in the manchette and head shaping were observed in KIF3A-depleted mice. We also identified cytoplasmic dynein 1 and GOLGA3 as novel interaction candidates for SPEF2 in the testis. Inhibition of dynein 1 activity in the manchette blocked the SPEF2 transport, suggesting its role in manchette-related transport. IFT20 and SPEF2 localization in the Golgi complex and the delayed appearance of IFT20 in the manchette in *Spef2* cKO suggests that SPEF2 functions as an adaptor in dynein 1-mediated transport in elongating spermatids. This study increases our understanding of the protein transport mechanisms required for the formation of functional spermatozoa.

Keywords: Intraflagellar transport, spermiogenesis, SPEF2, KIF3A

TIIVISTELMÄ

Mari Lehti
Mikrotubulusvälitteiset proteiinien kuljetusmekanismit spermiogeneesin aikana

Turun yliopisto, Lääketieteellinen tiedekunta, Biolääketieteen laitos, Fysiologian oppiaine, Molekyylilääketieteen tohtoriohjelma (TuDMM), Luonnonvarakeskus, Vihreä teknologia

Annales Universitatis Turkuensis, Medica-Odontologica, Turku, 2016

Solunsisäisen kuljetusmekanismin (intraflagellar transport, IFT) oikeanlainen toiminta on edellytys värekarvan ja siittiön hännän muodostumiselle. Kuljetusmekanismissa toimivat moottoriproteiinit, kinesiini-2 ja dyneiini ovat vastuussa proteiinien kuljetuksesta. Kuljetusmekanismin toiminta siittiön hännän muodostuksen aikana on vielä melko tuntematon. Tässä tutkimuksessa olemme pyrkineet selvittämään kuljetusmekanismin toimintaa poistamalla kinesiini-2 proteiinin alayksikön kinesiinin-kaltainen proteiini 3A:n (KIF3A) urosten sukusoluista. KIF3A proteiinin poisto aiheutti ongelmia siittiön hännän muodostuksen aikana. Siittiön hännän ydinrakenne, aksoneema, ei muodostunut sekä siittiön pään ympärille hetkellisesti ilmentyvä mikrotubulusrakenne, mansetti, oli epämuodostunut sekä sen poistuminen viivästynyt. Tunnistimme myös KIF3A:n kanssa toimivia proteiineja kiveksessä kuten KIF1:tä sitovan proteiinin (KBP) sekä meioosi-spesifin tuman rakenne proteiinin 1:n (MNS1).

Siittiön flagella proteiini 2:n (SPEF2) on näytetty ilmentyvän siittiön hännän muodostumisen aikana. Sen toiminta IFT kuljetusmekanismiin liittyvän IFT20 proteiinin kanssa on osoitettu aiemmissa tutkimuksissa. Tässä tutkimuksessa teimme urosten sukusoluspesifisen poistogeenisen hiirimallin SPEF2:lle ymmärtääksemme paremmin sen toimintaa siittiön hännän muodostumisen aikana. SPEF2 proteiinin poisto aiheutti ongelmia aksoneeman muodostuksessa, mansetti oli epämuodostunut sekä poisto viivästynyt, samoin kuten havaitsimme KIF3A poistogeenisellä hiirellä. Tunnistimme GOLGA3:n ja sytoplasmisen dyneiini 1:n SPEF2:n kanssa toimiviksi proteiineiksi. Osoitimme myös että dyneiini 1 moottorin toiminnan häiriö estää SPEF2 proteiinin kuljetuksen mansetissa. SPEF2 ja IFT20 proteiinien sijoittuminen Golgiin sekä IFT20 proteiinin viivästynyt paikantuminen mansettiin SPEF2 poistogeenisellä hiirellä viittaavat SPEF2 proteiinin mahdollisesta roolista toimia linkkinä dyneiini 1 moottorin ja IFT20 proteiinin välillä. Tämä tutkimus auttaa ymmärtämään proteiinien kuljetusmekanismeja siittiön kehityksen aikana.

Avainsanat: intraflagellaarinen kuljetus, spermiogeneesi, SPEF2, KIF3A

TABLE OF CONTENTS

ABBREVIATIONS

ATP	Adenosine triphosphate
BB	Basal body
BSA	Bovine serum albumin
CB	Chromatoid body
cKO	Conditional knockout
co-IP	Co-immunoprecipitation
CP	Central pair
CPC	Central pair complex
CTRL	Control
DA	Dynein arm
DAPI	4’,6-diamidino-2-phenylindole
DMSO	Dimethyl sulfoxide
DNA	Deoxyribonucleic acid
DRC	Dynein regulatory complex
ES	Elongating spermatid
FS	Fibroush sheath
IDA	Inner dynein arm
IF	Implantation fossa
IFT	Intraflagellar transport
IMT	Intramanchette transport
KBP	KIF1-binding protein
KIF3A	Kinesin-like protein 3A
KO	Knockout
LC	Longitudinal columns
LINC	Linker of nucleocytoskeleton and cytoskeleton
MNS1	Meiosis-specific nuclear structural protein 1
mRNA	Messenger ribonucleic acid
MS	Mitochondrial sheath
MTOC	Microtubule organizing center
NL	Nexin link
ODA	Outer dynein arm

ODF	Outer dense fibers
OMDA	Outer microtubule doublets of the axoneme
PAS	Periodic acid-Schiff
PBS	Phosphate buffered saline
PCD	Primary ciliary dyskinesia
PFA	Paraformaldehyde
PND	Postnatal day
RNA	Ribonucleic acid
RS	Radial Spoke
RT	Room temperature
RT-PCR	Reverse transcription polymerase chain reaction
RT-qPCR	Quantitative reverse transcription polymerase chain reaction
SPEF2	Sperm flagellar protein 2
TR	Transverse ribs

LIST OF ORIGINAL PUBLICATIONS

This thesis is based on the following original publications, which are referred to in the text by Roman numerals I-III:

I. **Lehti MS**, Kotaja N and Sironen A (2013)
KIF3A is essential for sperm tail formation and manchette function
Mol Cell Endocrinol. 2013 Sep 5;377(1-2):44-55

II. **Lehti MS**, Kotaja N and Sironen A (2015)
KIF1-binding protein interacts with KIF3A in haploid male germ cells
Reproduction. 2015 Sep;150(3):209-16

III. **Lehti MS**, Kotaja N and Sironen A (2016)
SPEF2 is involved in dynein-mediated transport in elongating spermatids
Submitted

The original publications have been reproduced with permission of the copyright holders.

1 INTRODUCTION

Understanding the complex process of sperm tail formation and its functions are essential for solving male infertility issues. The sperm tail is a specialized form of the cilium, a hair-like structure that points out of the cell surface. The function of cilia has been shown to be essential for life since cilia have multiple functions in different organs in the body. Motile cilia contain a 9+2 microtubule structure, where nine outer doublets surround the central pair of the microtubule. Inner and outer dynein arms are attached to the doublets and are responsible for cilia movement. Non-motile cilia contain only nine outer doublets and lack the structures required for cilia movement. For example, non-motile cilia in the kidney function as sensory organelles, and in the trachea, motile cilia play an important role in discarding the unwanted particles from the airways. Sperm tail and motile cilia axoneme share similar 9+2 microtubular structures. Thus, understanding the formation of the sperm tail will also help us understand the function of the cilia.

Animal models are widely used to understand male fertility since sperm tail development in vitro is still not established. Knockout mouse models for specific spermatogenesis-related genes are valuable tools for understanding protein functions and networks required for male fertility. Mouse and human spermatogenesis are conserved, and spermiogenic steps and cell types are similar. Thus, a mouse is an excellent model to understand human spermiogenesis and male infertility.

This thesis focuses on the complex process of sperm tail development, specifically to understand the function of the required protein transport mechanism. Since the axonemal structure of cilia and the sperm tail are identical, similar transport systems are likely to function in both. KIF3A is known to be an important player in intraflagellar transport (IFT) in a cilium, and SPEF2 has been known to be essential for sperm tail formation; however, these proteins specific roles during spermiogenesis are still not understood. By analyzing these proteins functions, we have been able to clarify the transport mechanism function during spermiogenesis. Results from this study reveal that a similar IFT mechanism, which functions in cilia, is essential for sperm tail formation. In addition to revealing the mechanisms of sperm tail formation, this study also underlines the importance of IFT-related genes in protein delivery in the manchette.

2 REVIEW OF THE LITERATURE

2.1 Spermatogenesis

Spermatogenesis, a complex process of sperm development, occurs in seminiferous tubules of the testis (Figure 1). It is a set of complex events, which starts with several mitotic divisions by spermatogonial cells and continues with chromosome duplications, genetic recombination, and finally a reduction of the chromosomes and genetic material via two meiotic divisions to produce haploid round spermatids. Round spermatids undergo dramatic metamorphosis to form mature spermatozoa with the head and tail (Hess, de Franca 2008).

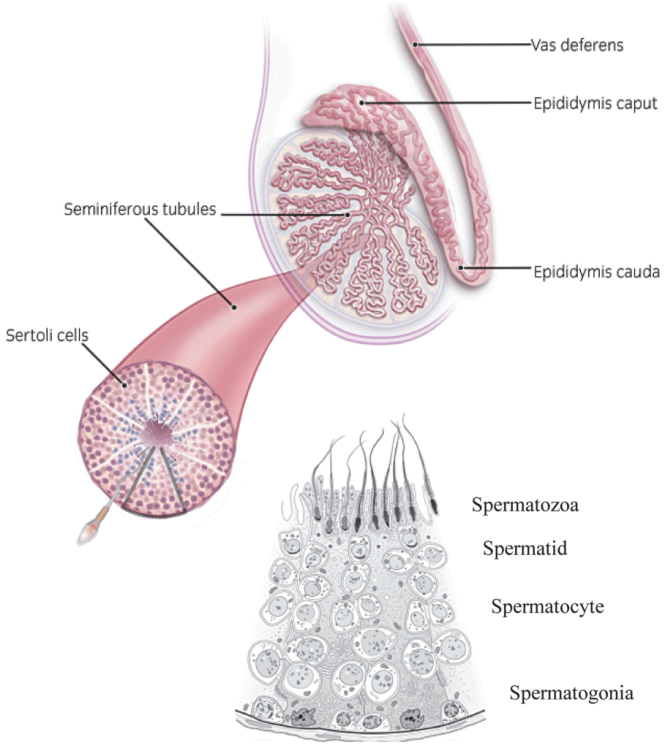

Figure 1. Spermatogenesis. Spermatogenesis occurs in the testis in seminiferous tubules. Spermatogonia divide by mitosis and give rise to spermatocytes. Spermatocytes go through meiosis and form haploid spermatids, which enter the complex transformation process to form elongated spermatids. Spermatozoa are released in the seminiferous tubule lumen and transported to the caput epididymis. During the epididymal transit, spermatozoa mature and are stored in cauda epididymis. Figure modified from (Samplaski et al. 2010).

In seminiferous tubules, spermatogonia reside next to the tubule membrane (Figure 1) and divide by mitosis to maintain the germ cell population. Sertoli cells are only somatic cells existing in the seminiferous tubules and are crucial for the spermatogenesis by nursing and regulating the environment of the germ cells (Hess, de Franca 2008, Franca et al. 2016, Griswold 1998). Four classes of spermatogonia can be recognized in mice: undifferentiated type A, which are early progenitor cells; differentiated type A (A_{1-4}), which are cells that have been committed to the differentiation pathway; and intermediate (In) and type B spermatogonia (B) (Hermo et al. 2010a). B spermatogonia divide by mitosis to form preleptotene spermatocytes (Pl), which enter meiosis I, resulting in secondary spermatocytes (Hermo et al. 2010a). Secondary spermatocytes undergo meiosis II and give rise to haploid round spermatids (Hess, de Franca 2008). Haploid spermatids begin a complex process referred to as spermiogenesis, where round spermatids are transformed into elongated spermatids. During this process acrosome is formed around the head, chromatin is condensed and the sperm tail is formed (Hess, de Franca 2008, Hermo et al. 2010b). Spermiogenesis can be divided into 16 steps, where in the first eight steps, spermatids appear round and axoneme elongation begins. In the following six steps, the manchette appears around the head and the head begins to achieve its typical hook-like shape. The accessory structures are formed throughout spermiogenesis and in the final two steps, sperm tail formation is finalized; at step 16, mature spermatozoa are released in the tubule lumen (Hermo et al. 2010b).

Spermatogenesis is organized in the seminiferous epithelium in a specific manner, where a given cross section contains a specific association of germ cells at different developmental stages (Hess, de Franca 2008, Ahmed, de Rooij 2009). These are called the stages of the seminiferous epithelial cycle and in mice, 12 stages can be recognized (Figure 2) (Hess, de Franca 2008, Ahmed, de Rooij 2009). At stage I, A spermatogonia, pachytene (P) spermatocytes, and steps 1 and 13 spermatids are present in the tubule lumen; stages II-III and IV contain A and In spermatogonia and P spermatocytes, steps 2-3, and 14, 4, and 15 spermatids appear respectively. At stages V and VI, A and B spermatogonia, P spermatocytes and step 5, 6, and 15 spermatids can be detected. At stages VII and VIII, A and A1 spermatogonia, Pl and P spermatocytes, steps 6, 7, and 16 spermatids and at stages IX and X, A2 spermatogonia, leptotene (L), and P spermatocytes and steps 9-10 spermatids are present. Stage XI, A3 spermatogonia, zygotene (Z) and diplotene (D) spermatocytes and step 11 spermatids are present in the tubule and finally at stage XII, A3 spermatogonia, Z spermatocytes, meiotic divisions and step 12 spermatids can be detected (Figure 2) (Hess, de Franca 2008, Ahmed, de Rooij 2009).

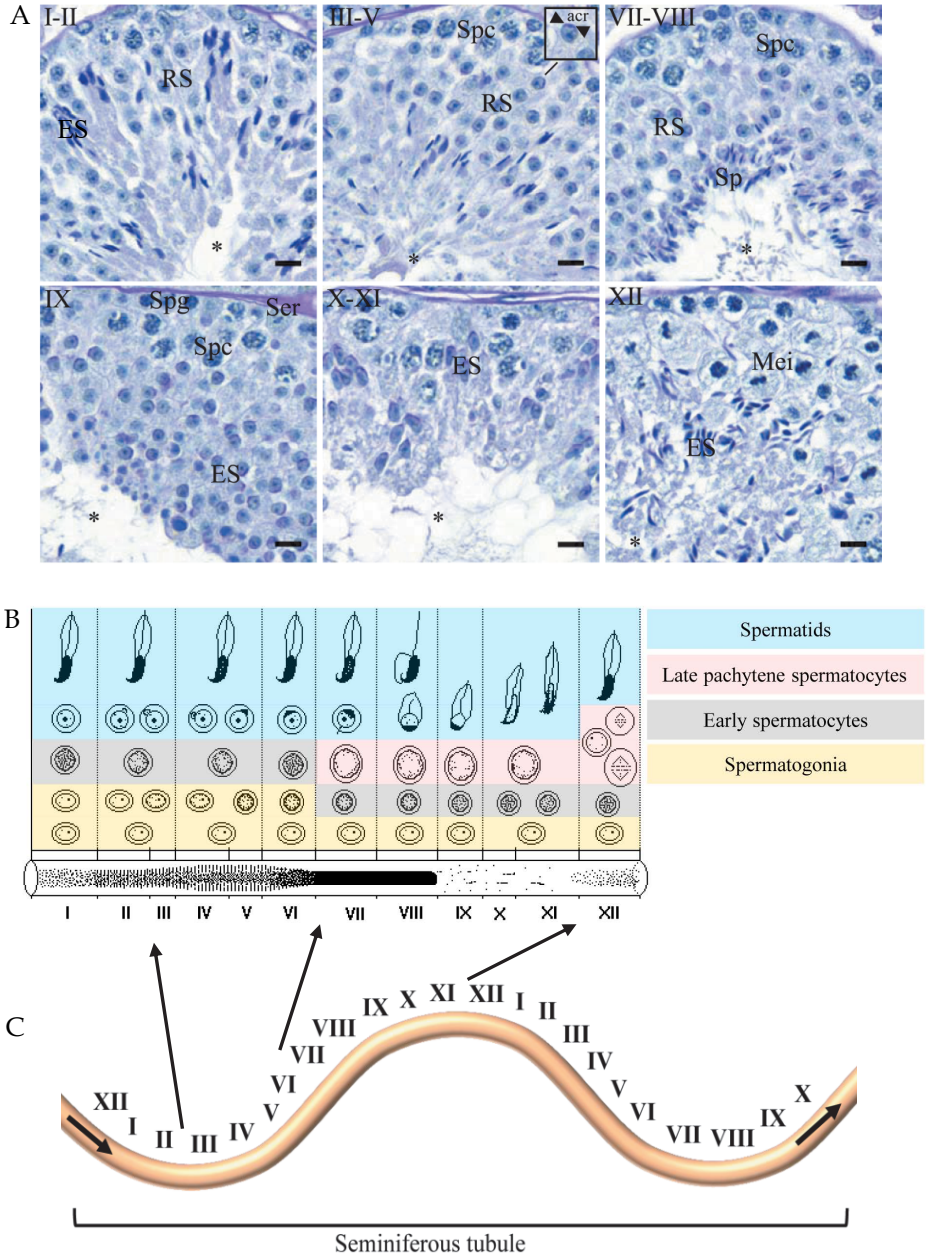

Figure 2. 12 stages of the seminiferous epithelial cycle in mouse. A. In stages I-II, both round and elongating spermatids are detected. Elongating spermatids locate in bundles near basal lamina. At stages III-V, the acrosome begins to flatten over the nucleus of round spermatids, and elongating spermatids are moving toward the tubular lumen. The acrosome continues flattening and covers almost two-thirds of the nuclei at stage VIII. At the stage VIII, spermatids are released into the tubular lumen. Round spermatids begin to elongate at stage IX and the

manchette appears. Secondary spermatocytes undergo meiosis to form haploid round spermatids at stage XII. RS: Round spermatid, Spc: Spermatocyte, acr: acrosome, Sp: Spermatid, Spg: Spermatogonia, Ser: Sertoli cell, ES: Elongating spermatid, Mei: meiosis, *: lumen, scale bar 1 μm. B. Graphical presentation of the stages of the mouse seminiferous epithelial cycle. C. Stages are following each other in order along the length of the seminiferous tubule. Figure modified from (Hogarth, Griswold 2010).

Different stages of the seminiferous epithelium can be identified from its cross sections (Figure 2). However, germ cells are not moving along the seminiferous tubule and stages can also be identified in consecutive order along the length of the tubule. This sequential order along the tubule length is called the wave of the seminiferous epithelial cycle (Figure 2) (Hess, de Franca 2008, Hogarth, Griswold 2010).

During the first wave of the seminiferous epithelial cycle, spermatogenic cells appear synchronously in the lumen of the tubule in a temporal manner. Newborn mouse testes contain only Sertoli cells and spermatogonia. At postnatal day (PND) 6, type A spermatogonia locate near the basement membrane and at PND8, both types of spermatogonia (A and B) are present in the tubules. Pl and L primary spermatocytes appear at PND10 in the tubule, and Z spermatocytes are present at PND12. At PND14, P spermatocytes are present and the seminiferous tubule has acquired lumen beginning from PND16. Secondary spermatocytes and round spermatids are increasing in number beginning from PND20 (Bellve et al. 1977). Elongating spermatids can be detected at PND28. A complete array of spermatogenic cells is present at PND35 (McKinney, Desjardins 1973).

2.1.1 Spermiogenesis

After meiosis, haploid round spermatids begin spermiogenesis, a process where the nucleus is condensed, the acrosome and sperm tail are formed, and excess cytoplasm is discarded (Hermo et al. 2010b). Spermiogenesis in mice can be divided into 16 steps (Figure 3, all stages and steps in this thesis describe mouse spermatogenesis unless otherwise stated) (Russell et al. 1990). At steps 1-8, the nucleus appears round and the acrosome flattens. Centrioles can be detected in the cytoplasm and the axoneme begins to elongate from the distal centriole (Turner 2006, Turner 2003). At steps 8-9, the manchette, a transient microtubular platform, appears around the distal part of the sperm head, participating in shaping the head and delivering the proteins to the developing tail (Hermo et al. 2010b). At steps 13-14, the manchette disappears (Lehti, Sironen 2016). Accessory structures of the sperm tail develop after the axoneme has been formed. At early spermiogenesis, the fibrous sheath (FS) starts to structure in the

principal piece (Irons, Clermont 1982); during midspermiogenesis, outer dense fibers (ODFs) develop to surround the axoneme in the principal piece and in the midpiece. In later spermiogenesis, mitochondria are assembled helically around the ODFs in the midpiece of the sperm tail. Finally, in step 16 spermatids, excess cytoplasm is discarded and spermatids are released into the tubule lumen (Turner 2003).

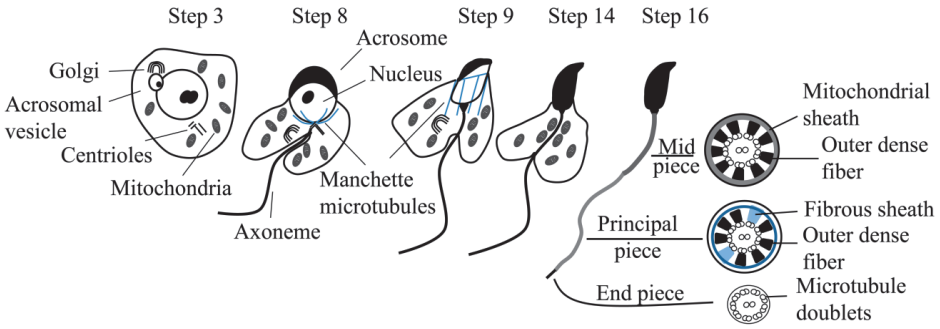

Figure 3. Overview of mouse spermiogenesis. At step 3, the acrosomal vesicle makes contact with the nucleus and starts spreading, covering over nearly half of the nucleus at step 8. Axoneme elongation begins at early spermiogenesis, originating from the distal centriole. Around steps 8-9, the manchette microtubules are assembled and sperm head shaping continues. The manchette has disappeared at step 14. FS formation begins at early spermiogenesis, ODF formation in midspermiogenesis, and finally the mitochondrial sheath assembles around the ODFs at late spermiogenesis.

2.1.2 Acrosome formation and the Golgi complex

The acrosome is a membrane-enclosed organelle surrounding the most anterior region of the sperm head (Figure 4). Acrosome biogenesis can be divided into four differentiation phases: the Golgi, cap, acrosomal, and maturation phases (Hess, de Franca 2008). In mice, the Golgi phase occurs at steps 1-3 of spermiogenesis (Hermo et al. 2010b). The Golgi complex participates in the initiation of acrosome formation and several Golgi-derived vesicles fuse together to form the acrosomal vesicle. Golgi-derived vesicles utilize a microtubular network to reach their destination (Moreno, Palomino & Schatten 2006). At the beginning of the cap phase during steps 4-5, the acrosomal granule makes contact with the nucleus, begins to flatten, and finally covers almost one-third of the nucleus at step 8. Simultaneously the Golgi complex begins to move to the opposite pole of the nucleus (Moreno, Schatten 2000). The acrosomal phase begins after step 9, when the elongating spermatid head forms a curved dorsal side and flat ventral side, and the acrosome moves over the ventral surface. The

acrosome maturation phase occurs at steps 15-16, when the nucleus still continues to condensate and the acrosome covers the whole ventral side of the head except the area which is connected to the tail (Hess, de Franca 2008).

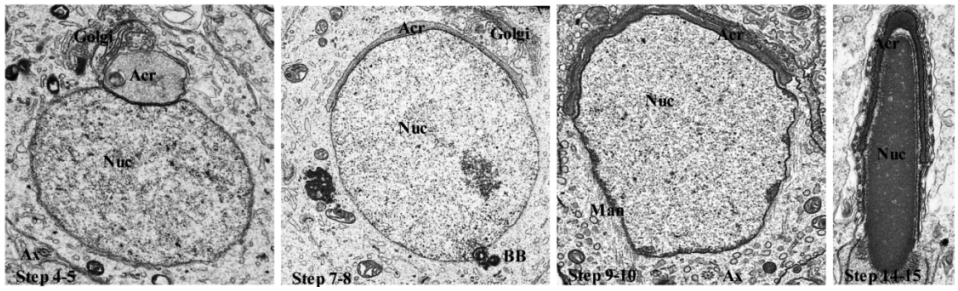

Figure 4. Acrosome formation. The acrosome appears first as a round shape at steps 4-5. It flattens and covers the nucleus opposite to the basal body (BB) at steps 7-8. At steps 9-10, nuclear elongation has been initiated and the manchette microtubules can also be detected. The acrosome is covering the condensed nucleus at steps 14-15. Nuc: nucleus, Acr: acrosome, Ax: axoneme, BB: basal body and Man: the manchette microtubules.

The developing acrosome is anchored to the surface of the nucleus by a cytoskeletal plate, the acroplaxome (Kierszenbaum, Rivkin & Tres 2003a). It consists of F-actin, Keratin 5, actin-based motor protein myosin Va, and Rab27a/b, a membrane-trafficking regulator (Kierszenbaum, Rivkin & Tres 2003b, Kierszenbaum et al. 2004). The acroplaxome is also thought to serve as a trafficking track for acrosomal vesicles. Studies with the HIV-1 Rev-binding protein (Hrb), a protein containing NPF motifs (Asn-Pro-Phe), mutant mouse have indicated the importance of the Hrb protein in acrosome formation. The Hrb protein locates in the cytosolic surface of Golgi-derived pro-acrosomal vesicles, and the lack of Hrb prevents vesicle fusion and blocks acrosome formation. In addition, in Hrb mutant mice, the acroplaxome lacks the protein Keratin 5, causing nuclear protrusion in pseudoacrosomal sites and round-headed sperm (Kierszenbaum et al. 2004, Kang-Decker et al. 2001). Furthermore, a mutation in the *Golgi-associated PDZ- and coiled-coil* motif-containing gene (*Gopc*) causes the generation of round-headed sperm that lack an acrosome. Golgi-derived vesicles fail to fuse and the acroplaxome leading edge, the marginal ring, formation was disrupted in *Gopc*$^{-/-}$ mice (Ito et al. 2004, Yao et al. 2002). These studies highlight the important role of the Golgi complex in acrosome formation.

2.1.3 Formation of the transient microtubular platform, the manchette

The manchette is a microtubular and F-actin-containing platform, which is transiently expressed during spermiogenesis. The manchette microtubules are attached to a perinuclear ring (Phillips 1980), locating adjacent to the marginal ring of the acroplaxome. The manchette microtubules seem to extend from the BB to surround the nucleus during steps 8-9 (Lehti, Sironen 2016). Microtubules reach out to the perinuclear ring and thereafter, dissociate and reach over the BB (Figure 5). The manchette is moving towards the tail and is disassembled during steps 13-14 (Lehti, Sironen 2016).

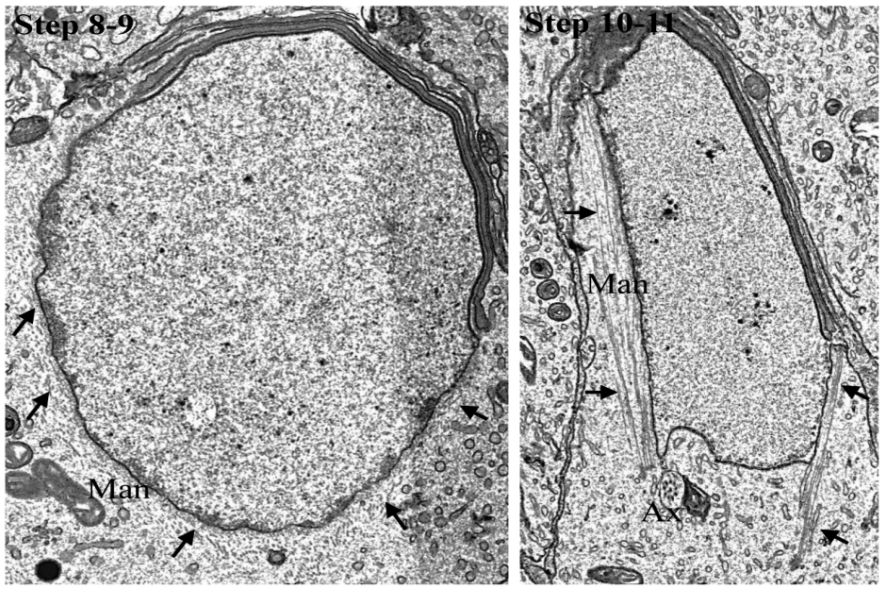

Figure 5. The manchette appears around the head. The manchette assembles around the head during steps 8-9. Microtubules dissociate from the BB at steps 10-11. Arrows are pointing at the manchette microtubules. Man: manchette, Ax: axoneme.

It is not completely understood how the manchette is constructed and from where its microtubules are originally nucleated (Lehti, Sironen 2016). Microtubules are composed of α- and β-tubulin heterodimers, which polymerize into long polarized filaments, wherein α-tubulin presents the minus-end and β-tubulin the plus-end of microtubules. The microtubule minus-end is connected to the microtubule organizing center (MTOC), which contains the most well-known nucleator, γ-tubulin (O'Donnell, O'Bryan 2014). The γ-tubulin forms a ring complex in the MTOC, where growing microtubule filaments can anchor themselves and stabilize (Teixido-Travesa, Roig & Luders 2012). During

spermiogenesis, γ-tubulin is found only from the centrioles. It has been shown that microtubule plus-end proteins, CLIP-170 (Akhmanova et al. 2005) and EB3 (Lehti, Sironen 2016), locate specifically near the perinuclear ring, suggesting that nucleation occurs at the BB. However, some studies propose that the manchette microtubules can nucleate from the perinuclear ring (Moreno, Schatten 2000). Periodic densities detected from the perinuclear ring have been suggested to function as MTOC for the manchette microtubules (Russell et al. 1991).

2.1.4 LINC complexes connect the manchette to the nucleus

The manchette is attached to the nuclear envelope via the linker of nucleocytoskeleton and cytoskeleton (LINC) complexes (Pasch et al. 2015), which have been shown to be important in linking the nucleus to the cytoskeleton in various cell types. LINC complexes are composed of bridges between the cytoskeleton and nuclear envelope, where interaction is formed by two transmembrane proteins, SUN and KASH (Crisp et al. 2006). In mammals, five distinct genes encode SUN proteins and of those, three are testis-specific: *Sun3* (Gob et al. 2010), *Sun4* (*Spag4*) (Shao et al. 1999), and *Sun5* (*Spag4L*) (Frohnert, Schweizer & Hoyer-Fender 2011). SUN proteins locate in the inner nuclear membrane and share a similar C-terminal SUN-domain (Sad-1/UNC-84), which interacts with KASH-domains (Klarsicht/ANC-1/Syne/homology) of KASH proteins. KASH proteins localize in outer nuclear membranes and are connected to the cytoskeleton (Pasch et al. 2015). Altogether, five KASH proteins are known: Nesprin 1 and Nesprin 2 are actin- and microtubule motor protein-interacting proteins (Zhang et al. 2001, Zhang et al. 2002), Nesprin 3 interacts with plectin (Wilhelmsen et al. 2005), Nesprin 4 is kinesin-binding (Roux et al. 2009), and dynein-binding KASH5 is meiosis-specific (Morimoto et al. 2012). Nesprin 1-3 and KASH5 are found in the testis. Sun4 has been localized specifically in the posterior side (the manchette region) of the sperm head and is present only in regions where cytoplasmic microtubules are in contact with the nuclear envelope. Implantation fossa (IF) and the sperm tail axoneme have been detected as negative for Sun4 (Pasch et al. 2015). Sun4 colocalizes with Sun3, and Sun3 has been shown to interact with Nesprin1 in the manchette (Gob et al. 2010). Sun4 knockout (KO) mice suffer from severe defects in head shaping and manchette detachment in addition to disorganized manchette microtubules (Calvi et al. 2015), supporting the theory that LINC complexes are involved in the manchette binding to the nuclear envelope.

2.1.5 Manchette removal

The manchette shapes the elongating spermatid head simultaneously with nuclear condensation by the zipper-like movement toward the neck region of the sperm (Toshimori, Ito 2003). The zipper-like movement continues until the perinuclear ring is no longer in contact with the nuclear membrane (Russell et al. 1991). Cytoplasmic dynein has been localized in the manchette in rat spermatids (Hall et al. 1992, Yoshida et al. 1994). During manchette removal, cytoplasmic dynein is located between the nuclear envelope and the manchette, suggesting it serves as a motor protein for the process (Yoshida et al. 1994). However, the exact mechanisms of manchette removal have not been studied. In addition to its role in head shaping, manchette movement along the head facilitates residual body formation and enables its removal during spermiation (Toshimori, Ito 2003).

2.1.6 Sperm tail structure

The sperm tail central structure, the axoneme, is similar to the axoneme of motile cilia. The sperm tail is a specialized form of cilia since the axoneme is surrounded by the accessory structures ODF, FS, and the mitochondrial sheath (MS) (Figure 6) (Turner 2003). Mature sperm tails can be divided into four parts: the connecting piece, midpiece, principal piece, and end piece. The connecting piece contains BB and connects the head and tail together. The midpiece contains all mitochondria found in the sperm and nine ODFs surrounding the axoneme. In the principal piece of the sperm tail, two ODFs are replaced by the longitudinal columns of the FS, which are connected to each other by transverse ribs (TR). The end piece of the sperm tail contains only the axoneme surrounded by the plasma membrane (Turner 2003).

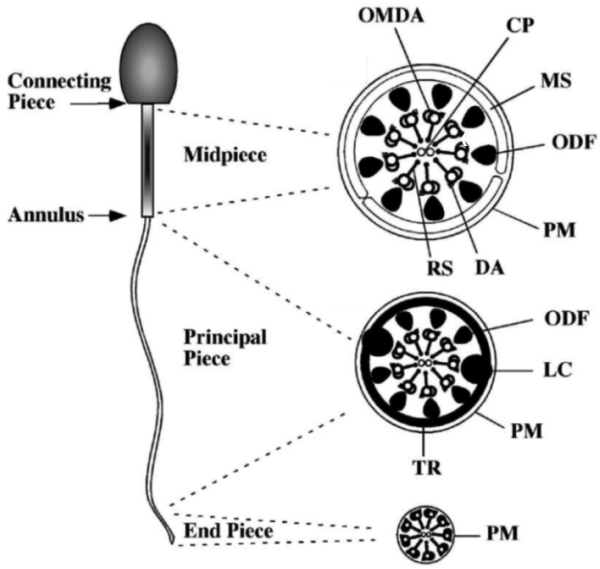

Figure 6. Structure of the sperm tail. Graphic illustration of the sperm tail structure. The connecting piece attaches the sperm tail and head. The axoneme runs through the whole length of the sperm tail. ODFs are found in the mid- and principal pieces. Longitudinal columns of the FS (LC) and TR are placed in the principal piece. All mitochondria found from the sperm are located in the midpiece. Figure modified from (Turner 2003). OMDA: outer microtubule doublets of the axoneme, CP: central pair, PM: plasma membrane, DA: dynein arm, RS: radial spoke, LC: longitudinal columns of the FS.

2.1.7 The sperm tail connecting piece

A pair of centrioles exists in the round spermatid cytoplasm. Axoneme elongation begins from the distal centriole at the beginning of spermiogenesis (Turner 2003). This pair of centrioles forms the connecting piece, a cone-shaped structure, which anchors the elongating sperm tail to the posterior pole of the nucleus (Figure 7). The capitulum is an electron-dense sheet in the connecting piece that associates with IF in the nuclear surface, connecting the tail to the nucleus. Centrioles are lost in mature sperm (Manandhar et al. 1999).

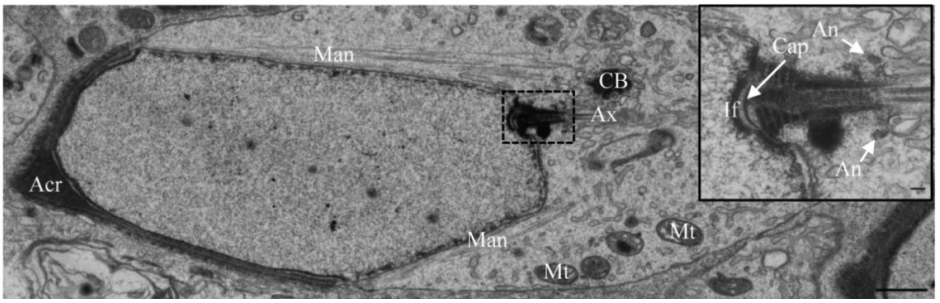

Figure 7. Step 11 spermatid. The connecting piece attaches the sperm tail to the head (encircled by dashed line, insertion). The manchette (Man) is a skirt-like structure surrounding the sperm head. Acr: acrosome, CB: chromatoid body, Mt: mitochondria, Ax: axoneme, If: implantation fossa, Cap: capitulum, An: annulus.

Defects in proteins involved in the connecting piece formation or function can cause head and tail disconnection. The SPATA6 protein is specifically expressed in the connecting piece of elongating spermatids. Microstructural studies have revealed SPATA6-specific expression in segmented columns and capitulum during spermatid elongation. Depletion of SPATA6 causes serious defects in the connecting piece and even its complete loss in steps 15-16 spermatids in addition to tail structure disorganization and acephalic sperm (Yuan et al. 2015). Depletion of the Centrosomal protein 131 kDa (Cep131) in Azi1/Cep131 KO mice causes misalignment of the centrioles in IF, and the sperm tail appears short and disorganized (Hall et al. 2013). Depletion of the centriolar protein Centrin 1 causes malformation of IF and BB degradation before axoneme formation in Centrin 1 KO mice (*Cetn1*$^{-/-}$) (Avasthi et al. 2013).

2.1.8 The annulus is a structural component and a diffusion barrier

The annulus is a SEPTIN-containing cytoskeletal ring around the axoneme. It appears in early spermiogenesis close to the connecting piece and causes invagination of the cell membrane around the axoneme. During spermatid elongation it migrates toward the principal piece of the sperm tail and anchors itself between the mid- and principal pieces (Guan, Kinoshita & Yuan 2009). The annulus has been thought to establish a diffusion barrier between these different membrane domains in addition to its function as a structural component of the sperm tail (Ihara et al. 2005, Kwitny, Klaus & Hunnicutt 2010). In mice, SEPTINs 1, 4, 6, 7, and 12 have been located in the annulus (Ihara et al. 2005, Kissel et al. 2005, Steels et al. 2007), and SEPT4 has been shown to be essential to the formation of the annulus and FS. *Sept4*$^{-/-}$ male mice are sterile due to immotile and morphologically abnormal spermatozoa. Depletion of SEPT4 causes absence of the annulus and FS, but the mitochondrial layer and ODFs

appear intact (Ihara et al. 2005). Furthermore, another study (Kissel et al. 2005) reports defects in the *Sept4* mutant mice mitochondria structure and variation in mitochondria size, resulting in defects in the normal precise arrangement of the mitochondrial layer. The migration of the annulus appears necessary for the transport of the residual body, since it is retained in the neck area instead of the distal midpiece near the annulus in *Sept4* mutant mice. The annulus functions as a membrane restriction barrier and has also been demonstrated using *Sept4*$^{-/-}$ mutant mice, where BASIGIN localization was distributed (Kwitny, Klaus & Hunnicutt 2010). In wild type mice, BASIGIN localizes in the principal piece in spermatozoa isolated from the caput epididymis, and in transition through the epididymis, BASIGIN translocates to the midpiece of the cauda sperm (Saxena et al. 2002). However, in *Sept4*$^{-/-}$ mutant mice, BASIGIN was present along the whole length of the sperm tail.

2.1.9 The cytoskeleton of the sperm tail: the axoneme

The axoneme of the sperm tail consists of a central pair (CP) of single microtubules (C1 and C2) surrounded by nine outer doublets of microtubules (Figure 8). Microtubule doublets contain two units of microtubules; A-tubules are round and complete and B-tubules are C-shaped, associating with the A-tubule. Both tubules are formed dimers of α- and β-tubulin (Hermo et al. 2010c). Axonemal microtubules are very stable since they contain high amounts of acetylated tubulin (Linck, Chemes & Albertini 2016). Dynein arms (inner dynein arms [IDA] and outer dynein arms [ODA]) project out from tubule A toward the adjacent doublet B-tubule. Doublets are connected to each other via nexin links (NL). Nexin locates between A- and B-tubules and is also a member of the dynein regulatory complex (DRC) of the IDA (Hermo et al. 2010c, Heuser et al. 2009). The A-tubule connects to the CP of microtubules established by radial spokes (RS). RS participates in motility by sliding past CP, transiently interacting with tubules. Phosphorylation and dephosphorylation regulate this brief interaction (Linck, Chemes & Albertini 2016).

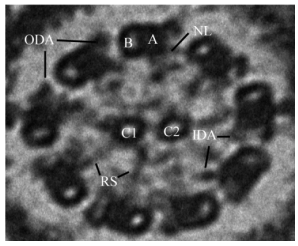

Figure 8. Structure of the sperm tail axoneme. Nine outer doublets surround the CP in the axoneme. Outer doublets contain A- and B-tubules, which are connected via NL. RS establish the connection between outer doublets and the CP. IDA and ODA are participating in the motility.

2.1.10 Defects in sperm axoneme formation

During spermiogenesis, the axoneme is the first sperm tail structure established. Defects in axoneme formation or structure often lead to overall failure of tail formation. Understanding sperm tail axoneme formation can be based on studies of the ciliary axoneme formation. Defects in ciliary axoneme formation cause primary ciliary dyskinesia (PCD), with various symptoms that include respiratory problems, situs inversus, and infertility (Praveen, Davis & Katsanis 2015). Unfortunately, detailed analysis of the function of PCD-causing genes during sperm tail formation is poorly studied. Several hundred genes are required for assembly of the axoneme, and some of them are known to affect male fertility. Most of the causative PCD genes with reported effects on spermatogenesis are related to the dynein arms. For example, defects in dynein axonemal assembly factor 2 (DNAAF2) and Leucine-Rich Repeat-Containing 6 (LRRC6) have been reported to be essential for cytoplasmic assembly of the ODA and IDA (Kott et al. 2012, Omran et al. 2008) before their translocation to the axoneme. Mutations in these genes cause the absence of ODA and IDA, causing defective axoneme formation in motile cilia. PIH domain containing 3 (Pih1d3) has also been reported to be involved in the cytoplasmic assembly of the dynein complexes. Pih1d3 depletion causes sperm immotility since both ODA and IDA are absent and overall structure of the sperm axoneme is disorganized (Dong et al. 2014).

Defects in the axonemal ODA genes dynein axonemal heavy chain 5 (DNAH5) (Fliegauf et al. 2005) and dynein axonemal intermediate chain 1 (DNAI1) (Guichard et al. 2001) cause reduced sperm motility, although sperm axoneme structure appears intact (Zuccarello et al. 2008). IDA-related coiled-coil domain-containing proteins 39 (CCDC39) and 40 (CCDC40) are involved in axoneme assembly and IDA function. Mutation of these genes causes reduced sperm motility and absence of IDA (Antony et al. 2013, Blanchon et al. 2012).

2.1.11 Structure of the central pair

The axoneme is a highly conserved structure across species and *Chlamydomonas reinhardtii* has been used as a model organism to understand the axoneme and central pair complex (CPC) formation. Recently the structure of the axoneme CPC has been visualized in *Chlamydomonas* (Figure 9). CPC contains two central microtubules (C1 and C2), which are linked to each other. From the C1 tubule, two longer (1a and 1b) and four shorter (1c-f) projections have been recognized, and from the C2 tubule, there are two longer (2a and 2b) and three shorter (2c-e) projections (Carbajal-Gonzalez et al. 2013).

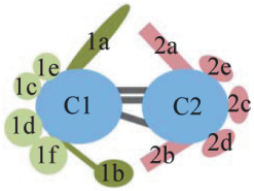

Figure 9. Simplified model of *Chlamydomonas reinhardtii* CPC. The central pair of microtubules consists of two longitudinal microtubules, C1 and C2, which are linked to each other. Both microtubules are connected to several projections (1a-f and 2a-e).

2.1.11.1 Defects in CP-related genes

Mouse models bearing a specific mutation in CPC genes have been useful in understanding differences between mammalian and *Chlamydomonas* axoneme structure and function. Mutation in the central pair complex 1 (CPC1) protein in *Chlamydomonas* causes reduced cilia beating frequency, and detailed analysis revealed that 1b projection was missing from the CPC (Mitchell, Sale 1999, Zhang, Mitchell 2004). The mammalian ortholog for *cpc1* is *Spef2*, which is expressed in the testis and other ciliated tissue (Ostrowski et al. 1999, Sironen et al. 2006, Sironen et al. 2010). The *Spef2* gene has several transcript variants and tissue-specific defects can be detected in SPEF2-mutated animal models (Sironen et al. 2006, Sironen et al. 2011, Finn, Evans & Lee 2014). SPEF2 depletion causes lowered beat frequency in tracheal epithelial cilia despite the fact that cilia structure appears normal. In the sperm tail, however, defects in axonemal structure are observed and one or both of the central microtubules are missing (Sironen et al. 2011). Thus, defects in sperm tail formation compared to ciliary structure may be more severe, indicating a more crucial role for specific protein isoform in the testis.

Mutation in a large, over 500-kiloDalton (kDa) polypeptide called Hydin results in the loss of C2b projection in mice (Lechtreck et al. 2008) and in humans (Olbrich et al. 2012), but also in *Chlamydomonas*, part of the C2c projection is missing (Lechtreck, Witman 2007). Hydin mutant mice suffer from hydrocephalus, impaired tracheal and ependymal cilia motility, and reduced beating frequency. In humans, depletion of Hydin causes PCD, and spermatozoa appear rigid and completely immotile (Olbrich et al. 2012).

Several Sperm-associated antigen (Spag) genes (*Spag6*, *Spag16,* and *Spag17)* have been shown to be important for CPC function. Deletion of the *Chlamydomonas pf16* ortholog for mouse *Spag6* causes impaired motility, and C1 projection is missing from the axoneme (Mitchell, Sale 1999, Smith, Lefebvre 1996). *Spag6*-deficient mice suffer from a variety of different symptoms, which are not limited to ciliated tissues, indicating that SPAG6 functions as a microtubule-associating protein. However, deletion of *Spag6*

causes infertility and defects in sperm axonemes, including missing central pair and disorganized ODFs (Sapiro et al. 2002, Sapiro et al. 2000).

PF6 in *Chlamydomonas* is required for the assembly of C1a projection and motility (Goduti, Smith 2012). *Spag17* is the mammalian ortholog for *pf6*, and its depletion in mice causes PCD. Ultrastructural studies have revealed the disappearance of one CP tubule and the loss of C1 projections in addition to other CPC abnormalities in tracheal cilia (Teves et al. 2013a, Teves et al. 2013b).

Pf20 is a *Chlamydomonas* ortholog for mouse *Spag16*. Mutation in *pf20* causes the disappearance of the whole CPC, since PF20 locates in the bridges between central tubules (Smith, Lefebvre 1996, Mitchell, Smith 2009, Smith, Lefebvre 1997). In the mouse, *Spag16* codes for two transcripts of sizes 35 kDa and 71 kDa: SPAG16S and SPAG16L, respectively (Zhang et al. 2004). Interestingly, SPAG16S is male germ cell-specific and SPAG16L is also expressed in cells with motile cilia. Disruption of both forms affects spermatogenesis (Zhang et al. 2004). However, depletion of only SPAG16L expression causes motility defects, but the axonemal structure of the sperm tail appears intact (Zhang et al. 2006). SPAG16S localizes in nuclear speckles at the beginning of spermiogenesis and regulates SPAG16L expression (Nagarkatti-Gude et al. 2011). Thus, it appears that there are testis-specific isoforms of ciliary genes, which may compensate for the loss of the ciliary variant.

2.1.12 Accessory structures of the sperm tail

2.1.12.1Fibrous sheath

FS has been thought to serve as a rigid support for the tail and participates in tail motility in addition to being a scaffold for metabolic- and signaling-related pathways (Turner 2006, Turner 2003). The sperm tail principal piece containing the FS covers almost three-quarters of the whole length of the tail. FS is composed of two longitudinal columns, which are attached to ODFs 3 and 8 in an anterior part of the principal piece. In the middle and posterior part of the sperm tail, longitudinal columns of FS replace ODFs and associate with outer microtubular doublets. Longitudinal columns decrease in size toward the end piece and are connected to each other by TR along the whole length of the principal piece. Formation of the FS continues during most of the spermiogenesis elongation phase, and formation of the longitudinal columns and TR occurs in a distal-to-proximal direction (Eddy, Toshimori & O'Brien 2003, Johnson et al. 1997). Thus, all proteins required for FS formation need to be transported to the assembly site.

Several proteins have been reported to localize in the FS of the sperm tail (Hermo et al. 2010c, Eddy, Toshimori & O'Brien 2003). Cyclic AMP-dependent protein kinase (PKA) anchoring proteins (AKAPs), PKA anchoring protein 82 (AKAP82 renamed AKAP4) (Carrera, Gerton & Moss 1994, Fulcher et al. 1995), AKAP3, and the A-kinase anchoring protein (TAKAP-80) (Mei et al. 1997) form the majority of protein content of the FS.

AKAP3 and 4 contain PKA RII and RI binding sites (Miki, Eddy 1999, Miki, Eddy 1998). AKAP4 binds the regulatory subunit (RII) in PKA proteins (Carrera, Gerton & Moss 1994, Visconti et al. 1997), which facilitates protein phosphorylation and regulates sperm tail motility. AKAP4 is expressed first as a precursor form in round spermatids (Fulcher et al. 1995). It is transported to the principal piece, where it is proteolytically modified to form mature AKAP4 (Johnson et al. 1997). AKAP4 has been shown to interact with AKAP3 (Brown et al. 2003). In AKAP4 mutant mice, less than 10% of spermatozoa were motile with reduced waveform, and none were able to generate progressive motility or hypermotility. Lack of motility was due to reduced thickness of the principal piece and the short tail. However, ODFs and the axoneme were unaffected. Ultrastructural studies suggested that FS structures begin to develop but fail to complete in the absence of the mature AKAP4. AKAP3 and glyceraldehyde 3-phosphate dehydrogenase-S (GAPDS) levels were also low in AKAP4 mutant mice, suggesting reduced glycolysis (Miki et al. 2002).

GAPDS is expressed in step 9 spermatids, but the protein appears in spermatids at steps 12-13. It specifically localizes in the FS, suggesting that it is involved in glycolysis and energy production and is therefore involved in sperm motility (Welch et al. 1992, Bunch et al. 1998). Depletion of GAPDS in the mice caused male infertility due to reduced sperm motility with no detectable progressive movement. In addition, glycolysis was impaired since ATP production was dropped by almost 90%. Interestingly, mitochondrial oxidative phosphorylation was retained, suggesting that glycolysis is the main energy source for sperm motility (Miki et al. 2004).

Calcium-binding tyrosine phosphorylation-regulated protein (CABYR), a protein with an RII binding domain, has also been identified in the FS of the sperm tail principal piece (Naaby-Hansen et al. 2002). CABYR contains two protein coding regions, CABYR-A and CABYR-B. CABYR isoforms form dimers and oligomers, which are involved in formation of the FS structure. CABYR is expressed first in step 11 spermatids and is transported to the FS during steps 15-16. The calcium-binding capacity of CABYR and increased calcium levels are required for sperm capacitation, a sperm maturation process required for fertilization (Breitbart 2002).

2.1.12.2 Outer dense fibers

ODFs begin from the connecting piece and can be found until near the proximal end of the principal piece. Nine ODFs form adjacent to axonemal outer doublets during midspermiogenesis, first as very thin filaments and then as gathering material later on. The ODF structure can be distinguished as a cortex composed of a single layer of globular units and the electron-dense medulla (Olson, Sammons 1980). ODFs are thought to provide support and elasticity to the motile tail, and they may enhance the strength of the waveform (Hermo et al. 2010c). The mRNA for ODF proteins is synthesized and stored in the cytoplasm and translationally regulated in later spermiogenesis after the transcriptional activity of haploid germ cells has been stopped. ODFs are resistant to detergents since they contain disulfide bonds. This has been a challenge in research trying to unveil the protein content of ODFs. However, there are studies that have successfully isolated and characterized multiple polypeptides from ODFs (Olson, Sammons 1980, Vera et al. 1984). ODF protein 1 (ODF1) is the most abundant protein in the ODF and is found from the medulla (Schalles et al. 1998, Burfeind, Hoyer-Fender 1991). Furthermore, ODF protein 3 (ODF3) (Petersen et al. 2002) and ODF protein 2 (ODF2) have also been detected in the testis (Schalles et al. 1998). ODF2 localizes in the cortex and medulla of ODFs and in the connecting piece. ODF2 is transcribed in both pachytene spermatocytes and round spermatids and is translated only in elongating spermatids (Schalles et al. 1998). ODF1 and ODF2 have been shown to associate through leucine zippers (Shao et al. 1997). SPAGS are ODF binding proteins, which are thought to be involved in ODF protein transportation to their destination (Kierszenbaum 2002b). SPAG4 has been identified as an ODF1 interacting protein (Shao et al. 1999), but it is also detected in the manchette and the axoneme. *Spag4* is transcribed in round spermatids and translated in elongating spermatids, similar to *Odf1*. *Spag5* is transcribed in both spermatocytes and spermatids, but in contrast to ODF2, SPAG5 is also translationally active in both of these cell types (Shao, Xue & van der Hoorn 2001).

2.1.12.3 Mitochondrial layer

The mitochondrial layer develops in later spermiogenesis. Mitochondria surround the axoneme and ODFs in the midpiece of the sperm tail. During spermiogenic steps 8-10, the mitochondrial matrix is less condensed and crescent-shaped. Some of these mitochondria migrate to the developing tail, and extra mitochondria are removed in the residual body. During steps 14-15, mitochondria translocate to the sperm tail midpiece, reduce their size, and coil

around ODFs (Meinhardt, Wilhelm & Seitz 1999). Mitochondrial layer formation can be divided into four phases. During phase one, mitochondria are round and assemble in four arrays circulating around the flagellum. During phase two, mitochondria become crescent-shaped and elongate, protruding between surrounding mitochondria in adjacent arrays. During phase 3, mitochondria continue to elongate and almost surround the ODFs. Finally, during phase four, mitochondria are rod-shaped and surround the flagellum, forming left-handed double helixes (Ho, Wey 2007).

SPERGEN-1 (also known as SPATA19) has been suggested to play a role in mitochondria cluster formation during midpiece formation. SPERGEN-1 contains an N-terminal mitochondrial targeting signal (Doiguchi et al. 2002) and specifically localizes to mitochondria in elongating spermatids and to the mitochondrial membrane in mature sperm in rat and mouse testes (Doiguchi et al. 2002, Matsuoka et al. 2004). Kinesin light chain 3 (KLC3) has been shown to associate with mitochondria (Bhullar et al. 2003) and ODFs (Zhang, Oko & van der Hoorn 2004) in rat testes. Studies with KLC3ΔHR-GFP mutant mice, which lack the ODF binding domain in the KLC3 protein, have shown mild defects in midpiece formation. Mitochondria were assembled in multiple layers or were unevenly divided around the ODFs. Thus, it can be speculated that KLC3 functions as a bridging molecule between mitochondria and ODFs (Zhang et al. 2012). In addition, selenoprotein GPX4 has been shown to act as a structural protein stabilizing the mitochondrial layer (Ursini et al. 1999).

2.2 Intraflagellar transport

Cilia and flagella lack protein translation machinery. All proteins and molecules required during cilia and flagella elongation have to be transported to the site of assembly and maintenance (Johnson, Rosenbaum 1992). IFT is the process whereby proteins and signaling molecules are transported to cilia and flagella. It utilizes axonemal microtubule outer doublets as tracks for motor proteins kinesin-2 and dynein 2 (Figure 10) (Hou, Witman 2015). Kinesin-2 is a plus-end directed motor protein carrying cargos toward the tip of the flagellum, and dynein 2 is a minus-end directed motor protein responsible for the transport back to the cell body. Dynein 2 and kinesin-2 bind large IFT-A and -B complexes, respectively. IFT complex A consists of 6 IFT proteins, and IFT complex B has 16 (Figure 10) (Lechtreck 2015). These IFT complex proteins form supramolecular structures and function as a link between the motor protein and the cargo.

Several studies have pointed out the importance of a functional IFT since dysfunctional transport causes failure in the formation of cilia or ciliary loss after

assembly (Davenport et al. 2007). For example, full deletion of the kinesin-2 subunit KIF3A causes abnormalities in left-right determination during development and embryonic lethality due to lack of cilia (Marszalek et al. 1999). IFT complex B IFT74 and -81 have been shown to interact directly with tubulins, and IFT81 interaction with the tubulin has been shown to be essential for cilia formation (Bhogaraju et al. 2013).

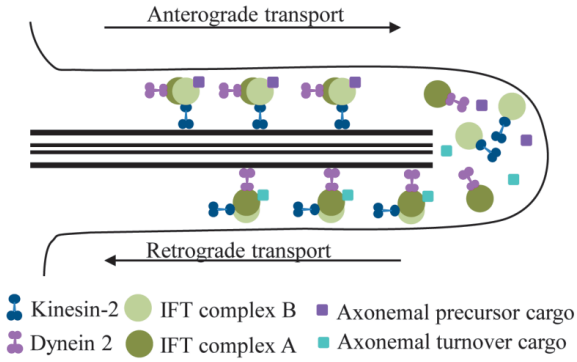

Dynein 2	Kinesin-2	
IFT complex A	IFTcomplex B	
IFT144	IFT172	IFT54
IFT140	IFT88	IFT52
IFT139	IFT81	IFT46
IFT122	IFT80	IFT38
IFT121	IFT74	IFT27
IFT43	IFT70	IFT25
	IFT57	IFT22
	IFT56	IFT20

Figure 10. Intraflagellar transport. Motor protein kinesin-2 transports particles needed for cilia assembly and maintenance along microtubular doublets just beneath the cell membrane. Retrograde motor dynein 2 restores spare particles back to the cell body. IFT-A consists of 6 IFT proteins and IFT-B contains 16 IFT proteins.

2.2.1 Microtubule-mediated protein transport in spermiogenesis

Two microtubule-based platforms, the manchette and the axoneme, are required for formation of the functional spermatozoa. Cargos utilizing motor proteins are transported along these microtubule structures. Since the axoneme of the sperm tail resembles the motile cilia axoneme, it suggests that similar protein transport mechanisms are operating during spermiogenesis. The manchette is involved in protein transport during spermatid elongation. Intramanchette transport (IMT) has been thought to share similar functions with IFT, since related molecular mechanisms and proteins are found in both microtubular structures (Kierszenbaum 2002a). Current evidence shows that the transport of proteins through the acroplaxome and the manchette is crucial for the development of the sperm tail and head shaping. However, little is known about the function of protein transport mechanisms during spermiogenesis.

Several proteins (e.g., HOOK1, p150Glued, GMAP210, and IFT88) have been localized to the acrosomal side of the nucleus before their migration through the acroplaxome and the manchette finally localizing in the connecting piece (Kierszenbaum et al. 2011, Kierszenbaum, Rivkin & Tres 2011). Several studies have suggested the manchette as an important route for transport of proteins required for formation of the spermatid axoneme and accessory structures.

Depletion of an important gene for ciliogenesis, *5-azacytidine induced gene 1* (*Azi1/Cep131*), causes major defects in spermatid head shaping and sperm tail formation (Hall et al. 2013). Cep131 has been shown to traffic along microtubules and concentrate on BB in studies with *Danio rerio* and *Drosophila melanogaster*. During spermiogenesis, it localizes in the acrosome at steps 10-12 and subsequently to the connecting piece, suggesting that it migrates through the manchette during spermatid elongation (Hall et al. 2013). The study of serine-threonine kinase Fused (Fu) has provided a link between IMT and tail accessory structure development. Fu is expressed in tissues containing motile cilia, and it plays a role in the assembly and maintenance of the axonemal central pair apparatus (Wilson et al. 2009). However, Fu mutant mice did not express defects in the sperm tail axoneme, but interestingly, FS was observed to be distorted and additional columns were present around the axoneme. Furthermore, Fu was localized in the acrosome, acroplaxome, perinuclear ring, and the manchette. It interacts with ODF1 and KIF27, which suggests its possible role in transporting and sorting cargos, such as components for sperm tail accessory structures (Nozawa et al. 2014).

Meiosis-expressed gene 1 (*Meig1*) has been thought to function in meiosis, but research with *Meig1* mutant mice revealed its role in the regulation of spermatogenesis and specifically its essential role in IMT. *Meig1* mutant mice suffered defects in head shaping and axoneme organization, and the manchette was disorganized or even absent (Zhang et al. 2009). MEIG1 interacts with the Parkin co-regulated (PACRG), which recruits MEIG1 to the manchette, and this complex is involved in SPAG16L transport to the growing flagella (Li et al. 2015). Furthermore, a not very well characterized gene, *leucine-rich repeats and guanylate kinase domain containing* (*Lrguk*), has been identified as essential for haploid sperm maturation. LRGUK isoform 1 (LRGUK-1) mutant mice have been identified with acrosomal detachment, manchette disorganization and impairment of its movement, and defective axoneme elongation from the BB. LRGUK-1 depletion also affects the BB attachment to the nucleus. LRGUK-1 has been localized to all these structures and interacts with HOOK2. LRGUK-1 and HOOK2 are potentially transported as a complex in the acrosome-acroplaxome-manchette-tail axis (Liu et al. 2015).

2.3 Kinesin-like protein 3A

The heterotrimeric motor protein kinesin-2 contains non-motor unit kinesin-associated protein 3 (KAP) and two motor units KIF3A, which form a heterodimer either with kinesin-like protein 3B (KIF3B) or kinesin-like 3C (KIF3C). Homodimers or heterodimers between KIF3B and KIF3C are rare (Marszalek et al. 1999, Marszalek, Goldstein 2000, Yamazaki et al. 1996, Yamazaki et al. 1995, Yang, Goldstein 1998, Kondo et al. 1994). KIF3A motor protein domain locates in the NH_2 terminus, the proline-rich globular region near the COOH end, and in the middle locates the alpha helical domain (Kondo et al. 1994). The essential role of KIF3A in cilia formation has been shown in KIF3A-null mutants where embryonic nodal cilia were missing, causing defects in left-right determination and death at day 10 post coitum (Marszalek et al. 1999). Since KIF3A full KO models are lethal, the function of KIF3A has been studied with several tissue-specific KO models. KIF3A depletion in photoreceptors causes cell death and prevents cilia axoneme formation (Marszalek et al. 2000, Jiang et al. 2015). In tamoxifen-induced photoreceptor-specific KIF3A knockout mice, the axoneme fell apart beginning from the distal end (Jiang et al. 2015), suggesting a role for KIF3A in axoneme maintenance in addition to its role in axoneme assembly. In the kidney, depletion of KIF3A caused loss of cilia and defects in planar cell polarity (Patel et al. 2008). During spermatogenesis, KIF3A function is not understood, but its localization in rat testes has been shown. KIF3A has been detected in the manchette, in the cytoplasm of spermatids (Hall et al. 1992), in the neck region, in the flagellum (Miller, Mulholland & Vogl 1999), and in the trans-Golgi network in the Sertoli cells in rats (Johnson, Hall & Boekelheide 1996). Thus, previous studies have demonstrated that *Kif3a* depletion prevents IFT in ciliated tissues and is present in the testis.

2.4 Sperm flagellar protein 2

The importance of SPEF2 for male fertility was first detected in pigs. Infertility problems in the Finnish Yorkshire pig population were already described in 1987, and 11 years later it was a serious reproductive problem. The problem appeared as a decreased sperm count and short immotile sperm tails. Electron microscopy studies revealed several problems in the organization of the sperm tail. One or both central microtubules were missing or less than nine outer doublets were seen (Andersson et al. 2000). Further studies revealed *Spef2* as a disease-causing gene (Sironen et al. 2006, Sironen et al. 2002). A large 9000 bp insertion was identified within the intron 30, causing premature translation stop codon and lack of the protein product. Sequence analysis confirmed integration

of a long interspersed nuclear element-1 (LINE-1) into the *Spef2* gene (Sironen et al. 2007).

The SPEF2 protein has been localized in the wild type mouse testis in the Golgi complex, the manchette, the BB, the midpiece of the sperm tail, and in the Sertoli cells (Sironen et al. 2010). SPEF2 localization changed during epididymal transport, where in caput sperm, SPEF2 staining appeared scattered along the midpiece and concentrated to the distal part of the midpiece in the corpus. In sperm isolated from the cauda and vas deferens, SPEF2 staining was clearly observed only in the distal part of the midpiece (Sironen et al. 2010). Yeast two-hybrid analysis has revealed IFT20 as an interaction partner for SPEF2 (Sironen et al. 2010). Both proteins are detected in spermatids in the Golgi complex and the manchette in steps 10-12 and around step 14 in the BB (Sironen et al. 2010). After this step the IFT20 staining was lost. Mutations in the *Spef2* gene in the *big giant head* (*bgh*) mouse model caused PCD-like symptoms, including hydrocephalus, sinusitis, and male infertility. Detailed analysis revealed two-point mutations in the *Spef2* gene. The mutation in exon 3 causes glutamine substitution to lysine in the domain of unknown function (DUF), which may cause dysfunction of domain folding or function. The second mutation in the *Spef2* gene was identified in exon 28. This nonsense mutation causes a premature translation stop codon and nonsense-mediated decay of the RNA product (Sironen et al. 2011). Interestingly, the pig model did not suffer from any symptoms other than the male infertility problem, suggesting that the mutation in the *Spef2* gene exon 3 is responsible for the identified PCD symptoms in the mouse model.

SPEF2 plays an important role in tracheal epithelial cells as well as in *bgh* mutant mice. Ostrowski and colleagues have identified upregulated *Kpl2* gene expression in cultured rat tracheal epithelial cells in addition to other ciliated tissues, including the brain, testis, and lung (Ostrowski et al. 1999). The actual function of SPEF2 in tracheal epithelial cells was investigated in more detail in *bgh* mutant mice. The structure of cilia in tracheal epithelial cells was normal, but the beating frequency was dropped by about 17% compared to the controls, which caused sinusitis and mucus accumulation in the sinus cavity (Sironen et al. 2011).

Several isoforms of *Spef2* have been predicted, and these appear to have a tissue-specific expression (Ostrowski et al. 1999, Sironen et al. 2010). The mouse *Spef2* gene contains 43 exons. PCR analysis detecting exons 3-7, 37-43, and 6-43 revealed that all studied exons are expressed in the testis, and exons 37-43 and 3-7 were also expressed in the lung, brain, kidney, and liver. Interestingly, PCR product from exons 3-7 was shorter in other studied tissues than in the testis, and

sequence analysis revealed that exon 4 was testis-specific. During the first wave of spermatogenesis, *Spef2* regions are differentially expressed, suggesting that several isoforms are also present during spermatogenesis. PCR product from exons 6-43 was first expressed at PND14, exons 37-43 were already weakly detected at PND7, and intense expression appeared at PND21. Exons 3-7 were not detected until PND28 (Sironen et al. 2010).

The SPEF2 protein contains several predicted domains of known function (Figure 11) ((Sironen 2009), www.ensembl.org, www.ncbi.nlm.nih.gov). The calponin homology domain is thought to bind actin; however, in vitro studies were not able to confirm the interaction (Chan et al. 2005) and DUF is common with proteins involved in flagella function, e.g. sperm flagella protein 1 (SPEF1) (Chan et al. 2005), sperm associated protein 4 (SPATA4) and CPC1. The nuclear localization sequence (NLS) is required for nuclear/cilia transport. The EF-hand contains a helix-loop-helix structure and is known as a calcium binding site. The P-loop containing adenylate kinase (ADK) site may be involved in the conversion of adenine nucleotides.

Figure 11. Mouse SPEF2 predicted protein domains. The SPEF2 protein sequence is predicted to contain several regions corresponding to known domains. The IFT20 binding site locates near the C-terminus of the SPEF2 protein. The gray box indicates *Spef2* exons 3-5.

3 AIMS OF THE STUDY

The overall aim of this study was to clarify the function of the protein transport mechanisms in sperm tail development by elucidating the roles of two proteins, SPEF2 and KIF3A. The IFT kinesin KIF3A is a potential regulator of protein transport during spermiogenesis. However, its exact functions in sperm tail development and maintenance are poorly understood. *Spef2* is a gene that has been shown to be involved in sperm tail development. It can be hypothesized that IFT is required for protein delivery during spermatid elongation. This hypothesis was tested using KIF3A depletion as a model. The localization pattern of SPEF2 in differentiating spermatids and interaction with IFT20 suggests that it might also be involved in IFT and the delivery of tail components.

Specific Aims of the Study

- To study the role of IFT during sperm tail development by using a male germ cell-specific KIF3A knockout mouse model
- Characterize the role of SPEF2 during spermatogenesis by developing a male germ cell-specific SPEF2 knockout mouse model
- To identify novel interaction partners for KIF3A and SPEF2 and their possible roles in protein transport

4 MATERIALS AND METHODS

4.1 Ethical statement (I-III)

Mice used in experiments were sacrificed with CO_2 or cervical dislocation and tissues were collected for experiments. All mice were handled according to international guidelines to care and use of laboratory animals. Mice were maintained in specific pathogen free stage at Central Animal Laboratory of University of Turku. All experiments was approved by the Finnish Ethical Committee (licence 315/041003/2011/ and 2006-1206-Kotaja).

4.2 Generation of *Spef2* targeting vector (III)

Generation of the *Spef2*conditional knockout (cKO) mouse model is described in detail in III. Briefly, targeting vector was designed to produce both full and conditional knockout mouse models for *Spef2*. DsRed fluorescent protein and stop codon were surrounded by Frt sites and inserted after exon 3. LoxP sites were inserted before Frt site upstream from exon 3 and after exon 5. Targeting construct was electroporated into hybrid mouse embryonic stem cells (G4, 129S6B6F1) and cells were injected into C57BL/N6 mouse blastocysts. Chimeric mice were bred with Flp deletor mice to delete DsRed and stop codon to generate *Spef2* cKO mouse model.

4.3 Generation of KIF3A and *Spef2* cKO mouse models (I-III)

To generate male germ cell-specific mouse model for *Spef2*, mice carrying LoxP sites surrounding exons 3-5 were mated with mice carrying Cre recombinase under control of neurogenin 3 promoter (Ngn3Cre) (provided by Dr. Pedro L. Herrera, University of Geneva, Switzerland) (Korhonen et al. 2011, Desgraz, Herrera 2009). Neurogenin 3 expression is induced in postnatal male germ cells at PND5 causing floxing of the *Spef2* gene only in male germ cells. For genotyping we used primers detecting LoxP site before exon 3 (III, Figure 1A and B). For experiments we used *Spef2* fl/-;Cre (*Spef2* cKO) mice and control mice were *Spef2* fl/- (CTRL) or B6 (C57BL/6N).

To create male germ cell-specific conditional mouse model for KIF3A, Ngn3Cre mice were mated with KIF3A fl/fl mice carrying LoxP sites before and after exon 2. KIF3A fl/fl mice were purchased from Mutant Mouse Resource and Research

Centers (MMRCC, The Jackson Laboratory, Bar Harbor, ME, USA) (Marszalek et al. 1999, Marszalek et al. 2000).

4.4 Genotyping of the conditional knockout mouse models (I-III)

Mice were earmarked and DNA was isolated for genotyping PCR. Genotyping primers used to confirm Cre expression were for Ngn3Cre forward 5′-CCT GTT TTG CAC GTT CAC CG-3′ and reverse 5′-ATG CTT CTG TCC GTT TGC CG-3′ and for pTimer forward 5′-ACG GCT GCT TCA TCT ACA AGG-3′ and reverse 5′-TTG GTG TCC ACG TAG TAG TAG-3′. Primers for *Spef2* genotyping were forward 5'-GAT TCT TAA ATT TTG AGG CC-3' and reverse 5'-ATG CTG TTC AGT GGA TAA AA-3'. *Kif3a* primers used for genotyping were forward 5'- AGG GCA GAC GGA AGG GTG G-3' and reverse 5'- GGT GGG AGC TGC AAG AGG G-3'. cKO mice were selected for analysis based on the positive Cre and pTimer band and homozygosity for the *Spef2* or *Kif3a* fl allele containing the flox sites.

4.5 Gene expression analysis

4.5.1 RNA sequencing (I)

Total RNA from C57BL/6NHsd mouse testis at timepoints PND7, 14, 17, 21, and 28 was extracted using RNeasy Midi kit (Qiagen) and samples were prepared for Solid4 sequencing using commercial kits and protocols provided by Applied Biosystems. The sequence reads were aligned against the mouse reference genome (mm9 assembly) using the standard whole transcriptome pipeline and the colorspace alignment tool provided by Applied Biosystems and distributed with the instrument (LifeScope v2.1). Differential transcript expression analysis was carried out using the Cufflinks pipeline (Trapnell et al. 2012).

4.5.2 RT-PCR (I)

RNA was isolated from the mouse testis and reverse transcribed using oligo T primers and ImProm-II Reversed Transcription System (Promega) according to manufacturer's instructions. Specific primers for *Kif3a* were forward 5'-GCC GAT CAA TAA GTC GGA GA-3' and reverse 5'- AGC CCC GGT ACT GCT CGA AC-3'. Primers for the control gene Eef2 were forward 5'-GCT TCC CTG

TTC ACC TCT GAC TCT G-3'and reverse 5'-CCT TGC ACA CAA GGG AGT CGG T-3'.

4.5.3 RT-qPCR (II)

RNA from the whole WT mice testis was extracted and reverse transcribed as described above. Primers used for cDNA amplification were for Kbp_001 forward 5'-ACGTGCCAGAGCTTTACCAT-3' and reverse 5'-AAA AGC TCC CTG GCT TCT TC-3', Kbp_004 forward 5'-ATT GCC ACA GCA CAC TGA AA-3' and reverse 5'-CAT ATA CAT GCC CCC AAA CC-3'. For the housekeeping gene *Rpl13a* primers were forward 5'-AGG GGC AGG TTC TGG TAT TG-3' and reverse 5'-CCG AAC AAC CTT GAG AGC AG-3'. qPCR was performed using ViiA7 Real-Time PCR System in 96-well microtiter plates using Absolute qPCR SYBR Green ROX Mix (VWR, Radnor, PA, USA). 12,5 µl of Absolute qPCR SYBR Green Mix, 70 nM of primers and 100 ng of cDNA was used in qPCR amplification, which started with 15 min enzyme activation at +95˚C followed by denaturation at +95˚C for 15s, annealing at +60˚C for 30 s and extension at +72˚C for 30 s for 40 cycles. Raw data was analyzed using sequence detection software (Applied Biosystems, Thermo Fischer Scientific) and relative quantitation was performed with GenEx Software (MultiD, Göteborg, Sweden). The mean of triplicates was used to define ratio between target and reference gene. Differences in amplification efficiency were corrected by producing standard curve for each primer pair. Primer-dimer formations were not observed for selected primers.

4.6 Immunohistochemistry

4.6.1 Immunohistochemistry of paraffin embedded testis samples (I-III)

Testis and epididymis were dissected and fixed with 4% paraformaldehyde (PFA) or Bouin's solution at RT for 4-20h. After washes with 50 % and 70 % ethanol testis were embedded in paraffin and cut into 4 µm sections. PFA-fixed testis sections were deparaffinized and rehydrated before antigen retrieval in 10 mM sodium citrate buffer pH 6.0, 0,05% Tween 20 in pressure cooker at 120 ˚C for 20 min. Slides were let to cool down for 2 hours and washed in MQ water and PBS before entering immunofluorescence stainings. For histology, PFA fixed epididymis and Bouin fixed testis sections was deparaffinize, rehydrated

and stained with Mayer's Hematoxylin and eosin or Periodic acid-Schiff (PAS) staining according to general protocols.

4.7 Protein isolation and co-immunoprecipitation (I-III)

For co-IP and protein analysis adult and 4 week old testes were dissected and snap-frozen in liquid nitrogen. Proteins were isolated in lysis buffer using Ultra Turrax homogenizor and centrifuged 13000 rpm at +4˚C for 30 min. Protein concentration was measured using Bradford assay (Thermo Scientific). Protein G Dynabeads were coupled with protein-specific antibodies and negative control antibodies (anti-Rabbit IgG or anti-Mouse IgG) and co-IP was performed according to the manufacturers protocol (1003D, Thermo Fischer Scientific, Waltham, MA, USA). For KIF3A co-IP adult testes were decapsulated and released seminiferous tubules were minced in small pieces for incubation in collagenase solution in rotation at RT for 1h. Testicular cell suspension was filtered, first through 100 µm and then through 40 µm silk, before centrifugation and suspension into lysis buffer [50 mM Tris–HCl pH 8.0, 170 mM NaCl, 1% NP40, 5 mM EDTA, 1 mM DTT and protease inhibitors (Complete mini; Roche diagnostic)]. Cell lysate was sonicated 10 times in 30 s intervals and incubated on ice for 20 min before lysate clearance by centrifugation.

4.8 Mass spectrometry (I, III)

For mass spectrometric analysis proteins were separated in 4-20% gradient SDS-page gels and specific bands were detected using Silver Staining Kit (Thermo Fischer Scientific). Protein bands of specific interest were isolated from the gel for in-gel digestion and tryptic peptides were dissolved in 10 µl of 1% formic acid and 5 µl was submitted to LC-MS/MS analysis using LTQ Orbitrap Velos Pro mass spectrometer. Database searches were performed by Mascot search engine and Swissprot protein sequence database.

4.9 Western blot (I-III)

Proteins were separated in denaturing conditions in 10% SDS-page gel or 4-20% precasted gradient gels (Bio-Rad). Proteins were blotted onto hybond membrane and blocked in 5% milk in 0.1% Triton X-100 PBS at RT for 1 hour. Primary antibodies (Table 1) were diluted in 1% milk in 0,1% Triton X-100 in PBS and incubated at +4˚C overnight. Membrane was washed with 0,1% Triton X-100 in

PBS and incubated with secondary antibody [HRP linked anti-mouse/rabbit IgG (GE Healthcare Life Sciences, Little Chalfont, UK)] diluted in 1% milk in 0,1% Triton X-100 in PBS at RT for 1h. Bands were visualized using ECL Plus Western blotting detection system (Amersham Pharmacia, Piscataway, NJ, USA) and chemiluminescence signal was detected with LAS4000 (Fujifilm, Tokoy, Japan).

4.10 Electron microscopy (I,III)

Specific stages of seminiferous tubule segments, epidymal sperm samples or testis were fixed in 5% glutaraldehyde. Samples were treated with potassium-ferro-cyanide-osmium fixative and embedded in epoxy resin. Sections were stained with 1% uranyl acetate and 0,3% lead citrate. Preparations were visualized with JEM 100SX, JEM1200EX or JEM-1400 Plus electron microscopes.

4.10.1 Immunofluorescence (I-III)

All immunofluorescence staining was performed as described above unless otherwise stated. Antibodies used for stainings are listed in table 1. Slides were blocked with blocking buffer (10% normal donkey/goat serum, 3% bovine serum albumin (BSA) diluted in 0,05% Triton X-100 in PBS) at RT for 1 hour. Primary antibody was diluted in antibody dilution buffer (Adb, 3% normal donkey/goat serum, 1% bovine serum albumin diluted in 0,05% Triton X-100 in PBS) and incubated at +4˚C for overnight. Slides were washed three times using 0,1% Triton X-100 in PBS and incubated with secondary antibody diluted in Adb 1:500. Nucleus was stained with DAPI (D9542, stock 5 mg/ml, Sigma-Aldrich, St. Louis, MO, USA) diluted in 1:10000 in PBS for 5 min, washed in PBS and mounted with Prolong Diamond Antifade Mountant (P36970, Life Technologies, Carlsbad, CA, USA) or Mowiol 4-88 medium (Polysciences, Inc). Images were acquired using Leica DMRBE, Zeiss Axio Imager M, Zeiss 510 Meta (Carl Zeiss AG, Oberkochen, Germany) or 3i Spinning Disk Confocal (Intelligent Imaging Innovations, Gmbh, Göttingen Germany).

4.10.1.1 Immunofluorescence of Drying Down preparations (I-II)

Testes were dissected and decapsulated in PBS. Stage-specific drying down preparations were prepared as described previously (Kotaja et al. 2004). Briefly

specific stages of seminiferous tubule were cutted and transferred into 100mM sucrose. Tubule pieces were ripped apart and cells were released into the sucrose solution. Cell suspension was spread into the object slide containing fixing solution (1% PFA, 0,01 % Triton X-100 in PBS) and dried o/n in humified chamber. Following day slides were air-dried and stored at -80˚C or continued directly to immunofluorescence stainings. Before immunofluorescence, preparations were post-fixed with 4% PFA for 5 min and washed before quenching autofluorescence in 100 mM NH_4Cl for 2 min. Preparations were washed in PBS and treated in 0,2 % Triton X-100 in PBS for 2 min before blocking and antibody incubations.

4.10.1.2 Immunofluorescence of cryosections (II)

Testis were dissected and fixed with 4% PFA at RT for 4h, washed in PBS and incubated in 20% sucrose at +4˚C for overnight. Testis were dried, embedded in Tissue-Tek O.C.T Compound (Sakura Finetek USA Inc, Torrance, CA, USA) and frozen in dry ice chilled isopentane or after dissection testis was embedded directly to Tissue-Tek O.C.T Compound for freezing. Testes were stored at -80˚C. Before immunofluorescence sections were post-fixed with 4 % PFA for 5 min, washed and permeabilized with 0,2 % Triton X-100 in PBS for 3 min. Slides were blocked in 10 % BSA in PBS and antibodies were diluted in 3% BSA in PBS.

4.10.1.3 Immunofluorescence of sperm slides (I)

Cauda epididymis was dissected and placed in PBS. Small incisions were made to let spermatozoa swim out at +37˚C for 30 minutes time period. Released sperm were collected, washed twice in PBS, spread onto object slides, air dried and stored in -80˚C. Sperm slides were post-fixed in 4% PFA for 15 min, washed in PBS and permeabilised in 0,2% Triton X-100 in PBS for 10 min. Sperm slides were blocked in 10 % normal goat serum in PBS and antibodies were diluted in 3% normal goat serum diluted in PBS.

4.11 Seminiferous tubule culture (III)

WT mouse testis was decapsulated and seminiferous tubules were released into PBS. Different stages of spermatogenesis were distinguished based on the light absorption observed under the stereomicroscope. The manchette-specific stages

(IX-XI) were cut and cultured in DMEM with dynein activity inhibitor ciliobrevin D in final concentration of 200 µM for 3-6 hours. Control tubules were incubated with equal amount of DMSO diluted in DMEM. After treatment with inhibitor or DMSO, tubules were collected, placed on object slides and squashed with a cover slip to spread germ cells out from the tubule. When monolayer was formed object slides were dipped into liquid nitrogen and cover slip was removed. Slides were fixed with 100% acetone, air-dried overnight at RT before immunofluorescence or slides were stored at -80˚C.

Table 1. Antibodies used in experiments

antigen	company	catalog #	Species & type	Western blot	Drying down	Testis section	Cryo-section	Sperm slides	Squash	Used in
Acetylated tubulin	Sigma	T7451, clone 6-11B-1	Mouse monoclonal IgG2b		1:1000					I
AKAP82			Mouse		1:500					I
Alpha-tubulin	NeoMarkers	MS-581-P	mouse monoclonal	1:4000	1:1000	1:1000			1:1000	I, III
Alpha-tubulin Alexa 488	Invitrogen	322588	Mouse IgG1-kappa		1:500					I
CBE1	Santa Cruz	sc-162645	Goat polyclonal		1:100					I
DYNC1l2	Proteintech	12219-1-AP	Rabbit IgG	1:1000		1:600				III
Gamma-tubulin	Abcam	ab11316	Mouse IgG			1:1000				III
Golga3	Mancini et al 2000		Rabbit	1:1000						III
IFT20	Gift from G. J. Pazour		Rabbit			1:200				III
KBP	Abnova	H00026128-B01P	Mouse polyclonal	1:300	1:100		1:100			II
KIF3A	Thermo scientific	PAI-20240	Rabbit polyclonal	1:4000	1:1000		1:2000	1:200		I, II
KPL2 end	Sironen et al 2010		Rabbit polyclonal	1:300						III
Lectin HPA (AF488 conjugated)	Life Technologies	L11271	mouse		1:50					
MNS1	Zhou et al 2012				1:250			1:250		I
MNS1	SantaCruz	sc-138435	Goat polyclonal		1:100					I
PT-KBP	Protein Tech	25653-1-AP	Rabbit polyclonal	1:300	1:200					II
Rhodamine PNA AF580-conjugated	Vector Laboratories	RL-1072				1:15000				III
SPEF2	Sigma	HPA039606	Rabbit polyclonal						1:200	III
TSKS	Shang P et al 2010		Rabbit		1:500		1:500			II

5 RESULTS

5.1 KIF3A is required for spermiogenesis (I)

5.1.1 KIF3A localization in the mouse testis (I)

Immunofluorescence analysis of WT mouse testis sections revealed that KIF3A protein expression begins in early P spermatocytes. In spermatogonia and early spermatocytes, the KIF3A signal was very low or absent. The KIF3A-specific signal was detected in the cytoplasm of spermatids until step 14, and more detailed analysis of the WT mouse drying down preparations localized KIF3A in the BB, the axoneme, and the manchette. In mature sperm isolated from the cauda epididymis, the KIF3A-specific signal was detected in the principal piece of the sperm tail (I, Figures 1 and 2).

5.1.2 Generation of the KIF3A cKO mouse model (I)

To investigate the specific function of KIF3A during spermatogenesis, we generated a male germ cell-specific cKO mouse model for KIF3A by breeding a floxed *Kif3a* mouse (Marszalek et al. 1999) with a Neurogenin 3- (Ngn3) Cre^{+} expressing mouse (Desgraz, Herrera 2009). The genotype of the mouse was confirmed by PCR, where the *Kif3a* floxed allele produced 490 bp length and the WT allele produced 360 bp length PCR products (I, Figure 3A). Expression of Cre recombinase was confirmed by detecting specific bands for Cre and pTimer as described previously (Korhonen et al. 2011). The disruption of the *Kif3a* open reading frame and protein production was confirmed by analyzing the total proteins and RNA isolated from both WT and KIF3A cKO mouse testes. A clear reduction in the KIF3A protein and gene expression levels was confirmed in KIF3A cKO mouse testes (I, Figure 3B and C).

5.1.3 KIF3A cKO males are infertile (I)

KIF3A cKO mice presented normal health statuses and they grew normally to adulthood. However, KIF3A cKO male mice failed to conceive WT females. Vaginal plugs were observed, but no pups were born after a six-week mating period. Analysis of the KIF3A cKO mouse testis and epididymis revealed

enormous reduction in sperm production. Only a few sperm were observed in the cauda epididymis and all of them appeared morphologically abnormal.

Analysis of KIF3A cKO mouse testis sections revealed normal organization of the seminiferous tubules, and all 12 stages of the seminiferous epithelial cycle were identifiable. Spermatogonia, spermatocytes, and round spermatids appeared normal, and defects were first seen at stage IX in KIF3A cKO testis sections. The sperm head shape appeared abnormal and the manchette was elongated. In addition, the sperm tail was undetectable (I, Figure 4).

Detailed structural analysis using electron microscopy of stage-specific tubule segments and sperm isolated from the cauda epididymis showed a total lack of the axoneme and disorganization of sperm tail accessory structures. All components required for sperm tail construction appeared to be produced, and short microtubules, FS, and ODF components were observed, but all of them were mislocalized. In addition, the manchette was placed ectopically and the perinuclear ring was constricted around the head, causing its abnormal knob-like shape (I, Figure 6).

5.1.4 KIF3A has several novel interaction candidates in the testis (I)

To understand more deeply the exact role of KIF3A during sperm development, we set up a co-IP to identify KIF3A interacting proteins. We used anti-KIF3A as a fishing antibody to pull down KIF3A and its interacting proteins from the WT mouse testis lysate. Interaction candidates were separated in SDS page gel for identification in mass spectrometry. Importantly, the whole kinesin-2 complex including KIF3A, KIF3B (Yamazaki et al. 1995) and KAP (Yamazaki et al. 1996) was pulled down, indicating the specificity of the method. Several interesting interaction candidates were also detected: Meiosis-specific nuclear structural protein 1 (MNS1, Q61884), Spermatid-specific manchette-related protein 1 (SMPR1, Q2MH31), Enkur (Enkurin Q6SP97), Outer dense fiber 3 (ODF3, Q920N1), Coiled-coil domain-containing 11 (CCDC11, Q9D439), Coiled-coil domain-containing protein 105 (CCDC105, Q9D4K7), and protein FAM166A (FAM166A, Q9D4K5). These interactions were identified in all triplicate KIF3A co-IPs and negative controls were clean (I, Figure 7).

5.1.5 Expression of KIF3A interaction candidates in the WT mouse testis (I)

Using transcriptomic sequencing, we analyzed expression of all KIF3A interaction candidates during the first wave of spermatogenesis. Different

spermatogenic cell types appear in the tubule in a temporal manner; the first spermatogonia are present at PND7, early spermatocytes appear at PND14, and late spermatocytes at PND17. Round spermatids are formed at PND21 and fully elongated spermatozoa appear at PND28 (Bellve et al. 1977). For all of the identified proteins, expression increased later, during the first wave of spermatogenesis. The KBP interaction with KIF3A has been previously published (Alves et al. 2010). Enkurin (Sutton et al. 2004) and ODF3 (Petersen et al. 2002) have been localized in the sperm tail, specifically in the principal piece and ODFs, respectively. SMRP1 has been detected in the manchette (Matsuoka et al. 2004) and studies with MNS1 KO mouse models have revealed its essential role during sperm tail development (Zhou et al. 2012).

5.1.6 MNS1 was retained in the manchette in KIF3A cKO mice (I)

We studied MNS1 protein localization in WT and KIF3A cKO mouse drying down preparations using two different antibodies. One antibody recognizes the internal region and another recognizes the C-terminal part of the MNS1 protein. We colocalized MNS1 with KIF3A in the manchette and principal piece of the sperm tail in WT mice. MNS1 was detected also in the principal piece of the mature sperm tail isolated from the cauda epididymis. Moreover, we could detect MNS1 in the acrosomal region and in the perinuclear ring. Using MNS1 antibody recognizing C-terminal part of the protein, we detected specific signals in the acrosomal granule and near the marginal ring. Interestingly, we could observe that the MNS1 signal was retained in the malformed manchette and acrosomal region in KIF3A cKO mice in steps 11-12 spermatids, when the MNS1 signal was absent in the WT. However, the MNS1 signal detected in the acrosomal region, granule, and perinuclear ring was not affected in the KIF3A cKO mice (I, Figure 8).

5.1.7 KBP expression during mouse spermatogenesis (II)

One of the KIF3A interacting proteins was KBP. To investigate the KBP-KIF3A interaction, we first confirmed the interaction by co-IP using KBP as a fishing antibody. We pulled down proteins from the adult WT testis lysate and confirmed the presence of KIF3A in the eluate by Western blot (II, Figure 4).

To study the localization of the KBP in WT mouse testes, we performed immunofluorescence staining in cryosections and drying down preparations. We detected the KBP signal starting from step 5 round spermatids and the strongest

signal was present in steps 12-15. The KBP signal appeared as a bright dot locating near the BB, in the manchette, and the connecting piece of elongating spermatids. However, at steps 15-16, the elongating spermatids KBP signal was reduced dramatically (II, Figure 1F). The specific localization of the KBP was confirmed using another antibody against KBP (ptKBP). Both antibodies stained specifically the manchette and a dot near the BB in drying down preparations. Furthermore, ptKBP also stained the acrosome and midpiece of the sperm tail (II, Figure 2). Both KBP antibodies recognize the full-length form of the KBP; however, the immunogen used for KBP has been full-length KBP and for ptKBP amino acids 272-621, which may explain the differences detected in staining patterns.

Two isoforms of *kbp* (*kbp*_001 and *kbp*_004) were expressed in WT mouse testes. *Kbp*_001 presents a full-length form of the *kbp,* and its expression peaked at PND21 (II, Figure 1B). Protein levels also consistently increased during the first wave of spermatogenesis, beginning at PND21 and showing the highest expression in the adult testis at PND42. We also analyzed the *kbp* expression in the lung, heart, liver, and kidney. The highest *Kbp*_001 expression was detected in the testis and lower levels were expressed in the lung, heart, and liver. *Kbp*_004 appears to be expressed only in the testis. *Kbp* expression was not detected in the kidney (II, Figure 1C).

5.1.8 KBP localizes to the late chromatoid body (II)

The KBP signal localization in elongating spermatids resembled the so-called late CB that is an electron-dense cytoplasmic granule found specifically in elongating spermatids. CB is a ribonucleoprotein (RNP) particles-containing granule, which is moving in the round spermatids cytoplasm. It is transiently in close contact with the nucleus and the Golgi complex/acrosome (Meikar et al. 2014). CB function is related to RNA regulation and processing pathways (Kotaja, Sassone-Corsi 2007). It has been shown that CB loses its characteristic markers at step 9 and is functionally transformed to the late CB (Shang et al. 2010), which divides into a ring structure that surrounds the developing flagellum and satellite structure that remains in the cytoplasm. To confirm the localization of KBP to the late CB, we performed co-staining with and antibody against testis-specific kinase substrate (TSKS) that is expressed specifically in the late CB (Shang et al. 2010). Interestingly, the TSKS signal overlapped partly with the KBP signal, suggesting the KBP localization is associated with the late CB. In a closer view, using phase contrast microscopy and a KBP-specific signal, we could define the late CB satellite as a KBP positive structure (II, Figure 3).

5.2 In *Spef2* cKO mice spermiogenesis is disrupted (III)

5.2.1 Spef2 cKO mice express truncated SPEF2 protein (III)

We generated *Spef2* cKO mice to understand the function of *Spef2* during spermatogenesis. To confirm *Spef2* gene depletion in the *Spef2* cKO mouse testis, we isolated RNA for RT-PCR analysis. mRNA covering exons 1-3 was detected only from C57BL/6N (B6) samples. From RT-PCR amplifying exons 1-9, we detected specific bands for both B6 and cKO, but the band from the cKO appeared shorter. After sequencing the PCR product, we confirmed the absence of exons 3-5 in cKO mice but the *Spef2* gene reading frame after the deletion appeared intact (III, Figure 1C). Western blot analysis revealed a weak shorter SPEF2-specific band in the cKO mouse testis lysate, indicating that a truncated form of the SPEF2 protein was translated despite the absence of exons 3-5 (III, Figure 1D). The full-length SPEF2 was absent in the cKO testis.

5.2.2 Spef2 cKO mouse spermatogenic phenotype (III)

The overall organization of the seminiferous epithelium appeared normal in the *Spef2* cKO, and spermatogenesis proceeded normally until late spermiogenesis. The most dramatic defects were observed at the beginning of stage XII in step 12 elongating spermatids with clear abnormalities in head shaping. Furthermore, during the later stages IV-VIII, sperm tails were not detected in the tubular lumen. In addition, fewer condensed heads were seen in stage VII in the cKO mice (III, Figure 1E). Reduction in the number of elongating spermatids was supported by the findings from the cauda epididymis, where almost no sperm were found in the cKO mice. In contrast, CTRL mice cauda were filled with mature sperm (III, Figure 1F). More detailed morphological analysis of the elongating spermatids using phase contrast microscopy of stage-specific drying down preparations confirmed defects in head shaping and tail elongation. The cKO elongating spermatids had short sperm tails or no tails at all. Bent tails or several tails per spermatid were also observed (III, Figure 2A). The tail accessory structures failed to form in the cKO spermatids (III, Figure 2A).

Ultrastructural studies revealed severe defects during spermiogenesis in cKO mice. We studied stage-specific seminiferous tubule segments using transmission electron microscopy. In axoneme cross sections, the central pair was incomplete or missing (III, Figure 2E). The acrosome and Golgi appeared normal in all steps during spermiogenesis (III, Figure 2B). The manchette microtubules were

assembled correctly in cKO mice, but they were constricting the head, causing knob-like head shaping (III, Figure 3A). It also appeared that manchette clearance was delayed in cKO mice (III, Figure 3B). We were able to identify mitochondria, ODFs, and FS components, but they were totally misplaced in cKO (III, Figure 2F). Interestingly, we could observe two basal bodies in several elongating spermatids. First, duplicated basal bodies were detected in step 7 spermatids (III, Figure 2C and D).

5.2.3 SPEF2 interaction candidates in the testis (III)

To understand the protein network required for SPEF2 function during spermatogenesis, we performed co-IP and mass spectrometry analysis. As a protein source, we used four-week-old mouse testis to enhance the number of early elongating spermatids in the lysate. We were able to identify the SPEF2 protein in the IP samples, which confirmed the specificity of the antibody and function of the method. The negative control antibody did not recognize any identified SPEF2 interaction candidates. We identified several interesting interacting candidates for SPEF2, such as two members of the cytoplasmic dynein 1 complex and GOLGA3 (III, table 1).

5.2.4 Cytoplasmic dynein 1 interacts with SPEF2 (III)

We further studied the cytoplasmic dynein 1 interaction since we pulled down two members from the cytoplasmic dynein 1 complex, the heavy chain 1 and intermediate chain 2 (III, table 1). We used an antibody against DYNC1I2 for further studies since it has been suggested as the possible interaction site for cargo adaptors. First we confirmed the interaction using co-IP with anti-DYNC1I2 as a fishing antibody, followed by Western blotting with a SPEF2 antibody (III, Figure 4A). For identification of the interaction site we analyzed the DYNC1I2 localization in the CTRL mouse testes sections. DYNC1I2 specific signal was observed in the spermatocytes cytoplasm and in the manchette of elongating spermatids. In the manchette, DYNC1I2 localized only to the area covering the nuclear surface, while the manchette microtubules free ends reaching over the nucleus toward the tail were DYNC1I2 negative. The DYNC1I2 signal in cKO mice appeared similar to the CTRL (III, Figure 4B). Since both SPEF2 and DYNC1I2 proteins are localized in the manchette, we further analyzed the possibility of cytoplasmic dynein 1 function as a motor protein for SPEF2. We prepared IX-XI specific segments from seminiferous tubules of B6 testes and incubated them with or without the dynein activity

inhibitor ciliobrevin D. After 3 hours of culture, we collected tubules for squash preparations and continued with immunofluorescence staining. We observed a clear effect of ciliobrevin D and inhibited dynein activity on the SPEF2 protein localization. In the control tubule culture, SPEF2 staining was only covering half of the manchette surface, leaving the area adjacent to the perinuclear ring devoid of SPEF2 signal, while in ciliobrevin D-treated cells, SPEF2 localization was covering the total area of the manchette (III, Figure 4C).

5.2.5 Interaction with GOLGA3 may connect SPEF2 to the Golgi complex

Since we could detect several hits for GOLGA3 in the mass spectrometric analysis, we studied GOLGA3-SPEF2 interaction further. We confirmed the interaction with SPEF2 and GOLGA3 by co-IP and Western blotting (III, Figure 5B). GOLGA3 localized to the Golgi complex of spermatocytes and round spermatids and to the acrosome/acroplaxome in the CTRL mouse testis sections. However, GOLGA3 localization was not changed in *Spef2* cKO mice (III, Figure 5C and D).

5.2.6 IFT20 transport is delayed in the Spef2 cKO

IFT20 has been identified as an interaction partner for SPEF2 in the mouse testis (Sironen et al. 2010). We studied the localization of IFT20 in the CTRL and *Spef2* cKO mouse testis sections. IFT20 localized to the cytoplasm of stages IX-XII elongating spermatids and the manchette (III, Figure 6A and B). In addition, an IFT20-specific signal was concentrated in the Golgi complex area in spermatocytes and round spermatids (III, Figure 5A). In cKO spermatocytes and round spermatids, the SPEF2 specific signal was less intense at the Golgi complex and more SPEF2 was found in the cytoplasm. Furthermore, the expression of SPEF2 was greatly reduced in the cytoplasm of cKO step 9 elongating spermatids. Closer examination of elongating spermatids showed that the appearance of IFT20 in the manchette was delayed compared to the CTRL. In addition, the distribution of IFT20 in the manchette was affected in the cKO, and the IFT20 signal covered the whole area of the manchette compared to the restricted localization in the lower parts of the manchette in CTRL spermatids (III, Figure 6B).

6 DISCUSSION

6.1 KIF3A and SPEF2 are required for sperm tail axoneme formation

6.1.1 Axoneme formation is blocked in the absence of KIF3A

Formation of the sperm tail axoneme begins in early spermiogenesis in round spermatids and is thought to utilize IFT. However, the actual functions of the motor proteins and cargo delivery mechanisms have remained unsolved. In KIF3A cKO mice, axoneme formation is perturbed at the beginning of spermiogenesis.

The IFT88 protein is a member of the IFT-B complex, which is known to interact and co-operate with kinesin-2 in the cilia assembly. Interestingly, mice with defective IFT88 have defects in sperm tail axoneme formation. In *ift88*$^{-/-}$ mutant mice, axoneme formation is not completely blocked, but short axonemes was assembled in elongating spermatids, and in some cases extra single or doublets of microtubules were present around the short axoneme (San Agustin, Pazour & Witman 2015). This indicates that tubulin transport was affected, but not completely blocked. It has been shown that tubulin is most likely transported via interaction with IFT-B complex proteins IFT74 and -81 (Bhogaraju et al. 2013) into the elongating axoneme, and therefore IFT88 may be involved in the transport of other components required for correct axoneme formation (San Agustin, Pazour & Witman 2015). However, the depletion of IFT88 appears to disturb the IFT-B complex and possibly kinesin-2-related functions, which causes defects in axoneme formation. Results from the KIF3A cKO mouse model suggest that KIF3A functions as an important anterograde motor protein for IFT that enables the transport of tubulin and other proteins required for axoneme assembly (Figure 13).

6.1.2 Depletion of SPEF2 disrupts CP formation

Previous studies have indicated the SPEF2 protein essential role in male fertility and sperm development (Sironen et al. 2006, Sironen et al. 2011). Similar defects in axonemal formation were found in *Spef2* cKO mice compared to previous animal models. In haploid spermatids at the beginning of spermiogenesis, the outer doublets of the axoneme were formed, but CP was missing. Furthermore, the sperm tail accessory structures were not correctly formed and they appeared

disorganized in elongating spermatids. In the mature sperm, the flagellar structure was completely disrupted, indicating that an intact axoneme is required for sperm tail formation. Studies with *Chlamydomonas* have revealed that formation of the CP of the axoneme begins shortly after the outer doublets formation (Lechtreck, Gould & Witman 2013). IFT transports CP components toward the tip of flagella, where they associate together to construct the CP in a tip-to-base direction. CP deficiency in *Chlamydomonas* caused IFT20, -172, -81, -57, and dynein motor to accumulate in the axoneme and the flagella appeared shorter (Lechtreck, Gould & Witman 2013). In *Spef2* cKO mice, the absence of CP caused shorter sperm tail formation and IFT20 accumulation in the BB, without disruption of the axonemal outer doublets.

Spef2 is a PCD gene causing decreased cilia beating frequency in tracheal epithelial cells (Sironen et al. 2011). Detailed analysis, however, did not observe defects in the tracheal ciliary structure (Sironen et al. 2011). Depletion of *Spef2* ortholog *cpc1* in *Chlamydomonas* causes absence of C1b projection, disturbing CP formation, and reduction of flagella beating (Mitchell, Sale 1999, Zhang, Mitchell 2004). We have analyzed the CP structure in the SPEF2 full knockout (*Spef2* KO, unpublished data) mice tracheal cilia using EM-tomography. The results showed that C1b projection in *Spef2* KO mice was intact (Figure 12, unpublished data, in collaboration with Dr Hannah Mitchison and Dr Amelia Shoemark, University College London). This proposes that SPEF2 is required for intact CP structure in the sperm axoneme, but the effect in tracheal cilia is not obvious. Thus, SPEF2 may function in protein transport rather than as a structural component in tracheal cilia.

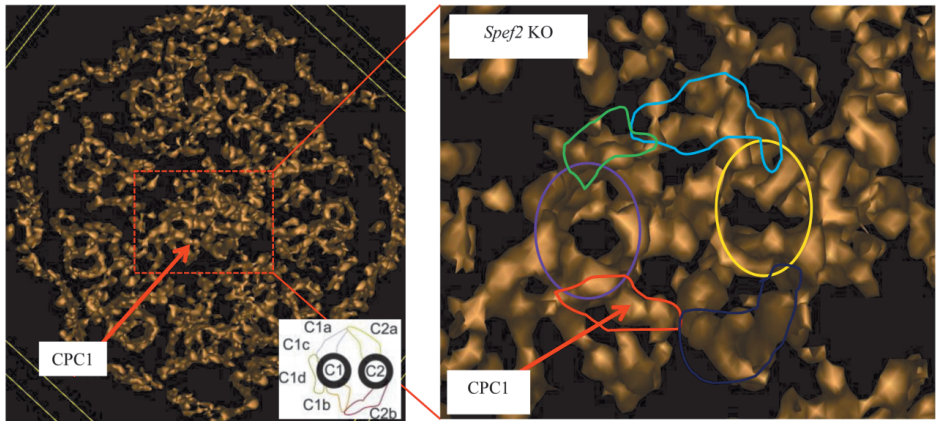

Figure 12. EM-tomography of *Spef2* KO mouse tracheal cilia. *Cpc1* is a ortholog for *Spef2*. CPC1 is a known structural protein of the C1b projection in the *Chlamydomonas* axoneme. In *Spef2* KO tracheal cilia, CP and C1b projection appeared intact. Graphical illustration of the CP from (Olbrich et al. 2012); EM-tomography figures were prepared by Hannah Mitchison and Amelia Shoemark, University College London.

6.2 KIF3A and SPEF2 function in protein transport during spermiogenesis

6.2.1 KIF3A and SPEF2 are involved in manchette-mediated transport

Both KIF3A and *Spef2* cKO mouse models demonstrate defects in manchette shape and function. Both proteins have been localized to the manchette, which suggests that KIF3A and SPEF2 have a role in manchette-related transport processes (Figures 13 and 14).

In KIF3A cKO mice, manchette formation in early elongating spermatids appeared unaffected, but in later steps it was ectopic, thick, and elongated. The manchette was still present in steps 13-14 spermatids, indicating its delayed clearance. These findings suggest that IMT resembles IFT and kinesin-2, and the functional IMT are required for the correct manchette function. This is further supported by the phenotype of *Ift88* mutant mice that closely resembles the phenotype observed in the KIF3A cKO. In mouse spermatids, IFT88 localizes in the Golgi complex, acrosome-acroplaxome, manchette, connecting piece, and tail. In *Ift88* mutant mice, spermiogenesis is disrupted, the sperm tail is not formed, and the manchette is abnormal, elongated, and ectopically assembled, causing a knobbed head shape (Kierszenbaum et al. 2011).

Similar to the KIF3A cKO, in *Spef2* cKO mice, manchette function was defective, causing an abnormal head shape. SPEF2 localization in the manchette, axonemal phenotype, and interactions with IFT20 and cytoplasmic dynein 1 complex suggest that SPEF2 is involved in manchette-mediated cargo transport during sperm tail formation. Cytoplasmic dynein 1 is a large and complex molecular motor driving cargo molecules toward the minus-end of the microtubules (Allan 2011). It has been localized in rat testes, specifically in the nuclear surface close to the manchette in elongating spermatids (Yoshida et al. 1994). Cytoplasmic dynein 1 complex protein DYNC1I2 was also localized in the manchette and between the manchette microtubules and nuclear surface. Its inhibition affected the distribution of SPEF2 in the manchette by allowing the localization of SPEF2 in the area close to the perinuclear ring. These results suggest that SPEF2 utilizes cytoplasmic dynein 1 as a motor protein for intramanchette trafficking (Figure 14).

Katanin p80-depleted mice (*Katnb1*$^{Taily/Taily}$) suffer from similar spermatogenic defects to *Spef2* cKO mice; sperm tail axoneme CP is missing in addition to some missing outer doutlets (O'Donnell et al. 2012). Furthermore, the manchette of *Katnb1*$^{Taily/Taily}$ mice was elongated and its clearance was delayed. The

perinuclear ring appears constricted, causing abnormalities in head shaping (O'Donnell et al. 2012). Katanin p80 is a regulatory subunit that forms together with the enzyme p60, a microtubule-severing complex. In *Chlamydomonas*, depletion of *pf15p* an ortholog for *Katanin p80* caused the absence of CP and paralyzed flagella (Dymek, Lefebvre & Smith 2004). Interestingly, Katanin p80 has been shown to bind cytoplasmic dynein (Toyo-Oka et al. 2005), highlighting the possibility that defects observed in *Katnb1*$^{Taily/Taily}$ mice may be related to defective transport in the manchette.

6.2.2 Sperm tail proteins are delivered through the manchette

Increasing evidence supports the functional interplay between IMT and IFT and the active transport of sperm tail proteins via the manchette to the site of a growing axoneme (Kierszenbaum 2002a, Li et al. 2015). KIF3A interaction with accessory structure proteins MNS1, ODF3, and Enkurin suggests that it could be involved in accessory structure delivery to the tail. MNS1 has been localized to the tail as a punctate staining in elongated spermatids (Zhou et al. 2012). In our studies, MNS1 colocalized with KIF3A in the manchette (Figure 13, I, Figure 8) and in the principal piece of elongating spermatids. In addition, MNS1 was also present in the acroplaxome (Figure 13). MNS1 has a role in sperm tail formation, as demonstrated by short and immotile sperm tails in MNS1 mutant mice (Zhou et al. 2012). Depletion of KIF3A caused a delay in the transport of MNS1 (and possibly other cargo particles) and its accumulation to the manchette. Defective IMT and overload of various cargo proteins in the manchette may also affect the elongation of the manchette and defects in its clearance.

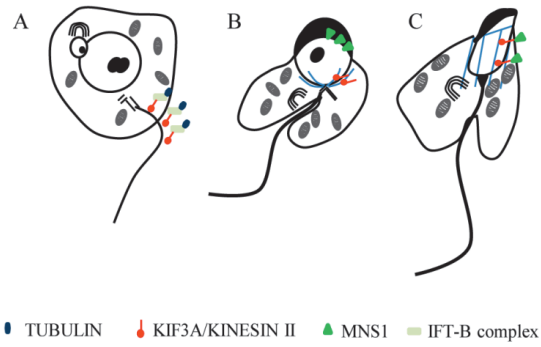

Figure 13. Hypothesis of KIF3A function during spermiogenesis. A. The KIF3A/kinesin-2 motor protein travels along the developing axoneme and transports tubulin to the site of axoneme assembly. B. During manchette formation in early elongating spermatids, KIF3A localizes along the microtubules and its interaction candidate MNS1 near the marginal ring. C. KIF3A is involved in MNS1 transport through the manchette.

The correct formation of the axoneme is required for accessory structure assembly. Since the axoneme is not formed in KIF3A cKO mice, we were not able to study the precise mechanism of the accessory structure formation. *Ift88*$^{-/-}$ mutant spermatids have a short axoneme, but the accessory structures appeared to be misplaced. FS was not detected along the tail and FS material appeared to be accumulated in the tips of the tail in *ift88*$^{-/-}$ mutants. ODF formation occurs in a base-to-tip direction, but the ODF fibers were not assembled correctly and were present in the cytoplasm of *ift88*$^{-/-}$ mutant mice (San Agustin, Pazour & Witman 2015). These results further support the possible involvement of kinesin-2 mediated transport in accessory structure formation.

6.2.3 SPEF2 is required for Golgi-derived transport

An interesting interaction candidate characterized for SPEF2 was GOLGA3. GOLGA3 has been shown to be essential for spermatogenesis (Banu et al. 2002, Bentson et al. 2013) and its depletion causes significant germ cell loss between days 15 and 18 during the first wave of spermatogenesis in *Golga3*^{repro27}mutant mice. During sperm tail elongation, *Golga3*^{repro27}mutant mice exhibited fused heads and tails, which may be caused by incomplete cell division. GOLGA3 locates in the Golgi complex and its interaction with GOPC has been indentified in HeLa cells (Hicks, Machamer 2005). *GOPC* -/- mice suffer from round-headed and acrosomeless sperm, suggesting that GOLGA3-GOPC interaction may be defected, causing vacuolization of the acrosome in the *Golga3*^{repro27}mutant. GOLGA3 depletion does not affect Golgi complex morphology and is probably required for cargo targeting and directing from the Golgi complex (Hicks et al. 2006, Williams et al. 2006). It is also shown that GOLGA3 recruits the dynein 1 motor protein to Golgi complex membranes and regulates Golgi complex motility (Yadav, Puthenveedu & Linstedt 2012). Because of the reported localization of SPEF2 in the Golgi complex, it is tempting to speculate that GOLGA3 may also recruit SPEF2 to the Golgi complex membranes and may be involved in cargo loading for dynein 1 mediated transport. Moreover, GOLGA3 localization in the acroplaxome may suggest its possible role in the Golgi complex-derived vesicle tethering toward the manchette microtubules (Figure 14).

SPEF2 has been shown to interact with IFT20, and they colocalize in the Golgi complex, manchette, and connecting piece of the sperm tail (Sironen et al. 2010). IFT20 has been linked to intracellular transport of compounds from the Golgi complex to cilia in addition to its role in IFT (Follit et al. 2006, Follit et al. 2009). GMAP210 anchors IFT20 to the Golgi complex membranes, and after vesicle

budding from the membranes, IFT20 marks them as ciliary cargo and transports them toward the ciliary base (Follit et al. 2008). In photoreceptors, IFT20 localizes in the BB of the connecting cilium and in the cytoplasm and membranes of the inner segment. It has been shown that inner segment membrane domains are involved in vesicle fusion and transport to the cilium. In this study we showed that in the absence of SPEF2, IFT20 protein was diffusely in the cytoplasm, indicating a defect in the accumulation of IFT20 in the Golgi complex. However, the localization of IFT20 in the Golgi complex was not completely blocked in *Spef2* cKO spermatocytes and round spermatids. In addition, the IFT20 signal was greatly reduced in the cytoplasm of early elongating spermatids, and its transport through the manchette was delayed. These results suggest that SPEF2 regulates the dynamics of IFT20, probably by functioning as an adaptor between IFT20 and cytoplasmic dynein 1 in Golgi-associated transport as well as in the manchette (Figure 14).

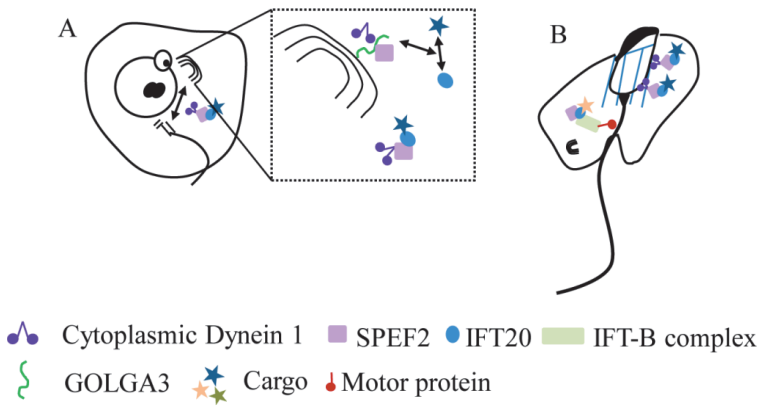

Figure 14. Hypothesis of SPEF2 function during spermatogenesis. A. SPEF2 interacts with GOLGA3, IFT20, and dynein 1 in the Golgi complex membranes. GOLGA3 recruits SPEF2 and dynein 1 to Golgi complex membranes, where they interact. SPEF2 functions as an adaptor for IFT20 and cargo proteins. B. Dynein 1 transports SPEF2 and IFT20 through the manchette toward BB. IFT20 interacts with the IFT-B complex in the BB and is transported together with SPEF2 to the elongating sperm tail.

6.2.4 The role of SPEF2 in late spermatocytes

We also observed duplication of the pair of centrioles in *Spef2* cKO mice. The overall structure of the centrioles appeared normal; however, the duplicated pair of centrioles was always attached together. The mechanism under this phenomenon is not clear and requires detailed analysis. The GOLGA3 has been

shown to be essential for late meiosis and correct cell division (Bentson et al. 2013). SPEF2 localized in the meiotic spindle and also in the BB (Sironen et al. 2010). However, we do not see a clear defect during meiosis in *Spef2* cKO mice. It has been shown that proteins involved in meiosis can cause very mild defects, resulting in only a decrease in the number of haploid spermatids (O'Donnell et al. 2012). Since at least one isoform of SPEF2 is present in the meiotic spermatocytes (Sironen et al. 2010), and both GOLGA3 and SPEF2 localize in the spermatocytes Golgi complex, it raises an intriguing thought that SPEF2 may be involved in Golgi-derived cargo transport during meiosis and is involved in centriole duplication, causing the identified BB defects in *Spef2* cKO mice.

6.3 SPEF2 has isoform-specific functions

Previous studies have indicated that SPEF2, specifically the 3' end of the *Spef2* gene, has an essential role in male fertility and sperm development (Sironen et al. 2006, Sironen et al. 2011). Our aim was to ablate the 5' end of the *Spef2* gene and protein expression during spermatogenesis by deleting exons 3-5. When comparing previous *Spef2* animal models (the *bgh* mouse model and the pig model) with the *Spef2* cKO mouse model generated in this study, similar defects in sperm tail formation were observed. Sperm tail formation was defected, including the lack of CP in the axoneme and assembly of the tail accessory structures. However, in contrast to other *Spef2* mutant animal models, *Spef2* cKO suffered from defects in manchette function and sperm head shaping. Since the *Spef2* gene has various isoforms, the depleted exons from the 5' end may also disrupt other *Spef2* isoforms in addition to the full-length form of the *Spef2* gene. This may explain the phenotypic differences in spermatogenesis between animal models, since in the pig and *bgh* models the 3' end of the *Spef2* gene was depleted.

Previous studies have also shown different expression patterns for specific *Spef2* gene exons during the first wave of spermatogenesis (Sironen et al. 2010). A faint expression of exons 37-43 was already detected at PND7 and peaked at PND21. This may suggest that the 3' end of the *Spef2* gene is important for the beginning of axoneme formation. *Spef2* gene exons 3-7 expression was prominent at PND28, when elongating spermatids appear in the tubular lumen. In *Spef2* cKO mice, exons 3-5 were depleted, which may explain the more serious and diverse defects detected, particularly in the elongating spermatid manchette.

In the *bgh* model, the *Spef2* gene contained mutations in exon 3 (missense) and in exon 28 (nonsense), and the pig model had a mutation only in intron 30 (nonsense). Besides defects in spermatogenesis, *bgh* mice also suffered from

hydrocephalus, sinusitis, and reduced tracheal epithelial cilia beating. Since the pig model did not suffer from symptoms other than spermatogenic defects, it can be hypothesized that defects in other tissues are caused by the mutation in exon 3. This is also supported by the results gained from the studies with *Spef2* KO, which has a stop codon after exon 2 (unpublished data). *Spef2* KO mice suffered from severe hydrocephalus and growth retardation and usually died at three weeks of age. It appeared that the hydrocephalus was more severe in *Spef2* KO mice than in *bgh* mice models, which might have been caused by complete deletion of the 5' end isoforms.

Several protein domains with known functions have been predicted based on the SPEF2 protein sequence (Figure 11). Two NLS, P-loop with ADK, and EF-hand domains may remain intact in the *Spef2* cKO. However, in SPEF2, functions of these domains have not been studied. DUF and calponin homology domain localize near amino-terminus, and both domains are disrupted in *Spef2* cKO mice. It has been shown that calponin homology domain containing proteins may be involved in regulating cytoplasmic dynein activity by binding dynein-dynactin complex (Olenick et al. 2016). Similar DUF domain has been predicted from SPATA4 and SPEF1 protein and both proteins have been implicated to cilia/flagella function. Depletion of SPATA4 caused decreased cilia number in retinal epithelial cells and increased number of BBs (Albee et al. 2013). SPEF1 has been detected from the sperm flagella as integral component (Chan et al. 2005), suggesting that similar DUF domain-containing proteins are involved in flagella or BB assembly or function. Defects detected in *Spef2* cKO mice suggest that the disrupted amino-terminus may cause problems in the function of the other protein domains. The full length form of SPEF2 appears to be required for correct sperm tail formation based on the previous studies and the observed defects in the cKO mice indicate that the truncated form is not able to rescue the sperm phenotype. However, complete understanding of the function of the SPEF2 domains and isoforms requires further studies.

6.4 KIF3A interacting partner KBP is a novel late CB marker

The exact function of the KBP protein has not been revealed in previous studies, but its interaction with kinesin motor proteins and microtubule destabilizing protein SCG10 has been established (Alves et al. 2010, Wozniak et al. 2005). KBP is involved in the axonal outgrowth in central and peripheral nervous systems in the zebrafish (Lyons et al. 2008). We identified KBP expression during spermatogenesis and confirmed its interaction with KIF3A. Interestingly, KBP has a specific localization in the late CB in addition to its colocalization

with KIF3A to round spermatids cytoplasm and the manchette. CB is an electron-dense granule that has been thought to serve as an RNA processing center in round spermatids. It contains multiple RNAs including mRNAs, long noncoding RNAs, and piRNAs, as well as a variety of RNA-binding proteins and proteins involved in RNA regulation (Meikar, Kotaja 2014). During spermiogenesis, the CB moves in close, associating with the nuclear membrane toward the connecting piece. At the onset of spermatid elongation, there are dramatic changes in CB composition and the majority of well-characterized CB components disappear and the CB is thought to be functionally transformed (Shang et al. 2010). The full protein composition of this late CB is still unclear, but it has been reported to contain testis-specific serine/threonine protein kinase 1 (TSSK1) and 2 (TSSK2) and TSKS (Shang et al. 2010). At this point, the late CB divides, forming a ring around the axoneme close to the annulus and the connecting piece and a freely moving satellite granule (Shang et al. 2010, Parvinen 2005). During midpiece formation, the late CB ring moves along the axoneme to the junction between the mid- and principal pieces, and it may be involved in mitochondrial layer formation (Shang et al. 2010, Chuma et al. 2009). Both CB-derived structures diminish in size during elongation and are removed in the residual body. KBP is most probably involved in microtubule-mediated functions (Alves et al. 2010, Drevillon et al. 2013) and thus may be involved in CB movement during later steps of spermiogenesis or may regulate microtubule related KIF3A transport in the manchette. The CB appeared fragmented in steps 11-14 spermatids of KIF3A cKO mice; however, this defect may be a secondary consequence of the serious defects during sperm tail development and manchette function. Further studies are required to understand if KIF3A is directly involved in CB integrity and to solve the role of KIF3A in CB function.

7 CONCLUSIONS

Correct sperm tail construction and function are essential for male fertility. To reveal protein networks and transport mechanisms required for functional spermatozoa, cKO mouse models for KIF3A and SPEF2 were generated. This study characterized the vital roles of KIF3A and SPEF2 during spermatogenesis and established their role in protein transport.

Major findings of this study:

1. IFT is required for sperm tail axoneme formation and manchette function

2. KIF3A is involved in protein transport via the manchette to the developing tail

3. KIF3A interacts with a novel late CB protein KBP and may regulate CB motility

4. SPEF2 is involved in sperm tail axoneme CP assembly and manchette function

5. Cytoplasmic dynein 1 is the motor for SPEF2 transport through the manchette

6. SPEF2 may be involved in Golgi-associated cargo transport

ACKNOWLEDGEMENTS

This study was carried out at the Department of Physiology, Institute of Biomedicine, University of Turku during the years 2010-2016.

My deepest gratitude goes to my supervisors Docent Anu Sironen, and Associate professor Noora Kotaja. I do not have words to describe how excellent supervisors you both are. I feel extremely lucky and privileged that I have had this opportunity to work with you both. First, I would like to thank Anu that you gave me this opportunity to work in the fascinating world of spermiogenesis. You have always believed in me and given me freedom to learn. Without your expertise, passion and supervision this thesis would have been impossible to do. I am grateful to Noora for your support. Your advices and ideas have been valuable for completing this thesis. No matter how busy you have been, you have always found time for me which I appreciate a lot.

Research Director Eleanor Coffey, and Professor Seppo Vainio, are acknowledged for reviewing this thesis and for giving comments and suggestions to make this thesis better. I wish to thank members of my thesis advisory committee, Professor Johanna Vilkki, Professor Jorma Toppari, and Research Director Eleanor Coffey, for their valuable advices during this process.

I wish to thank all past and present Professors, Docents, Researchers, and Postdocs from the Department of Physiology for creating supportive and collaborative environment. My deepest thanks goes to Ilpo Huhtaniemi, Marko Kallio, Jukka Kero, Harri Niinikoski, Lauri Pelliniemi, Matti Poutanen, Nafis Rahman, Manuel Tena-Sempere, Jorma Toppari, Annika Adamsson, Holger Jäschke, Christoffer Löf, Juho-Antti Mäkelä, Mirja Nurmio, Pirjo Pakarinen, Pia Rantakari, Adolfo Rivero-Müller, Suvi Ruohonen, Kalle Rytkönen, Niina Saarinen-Aaltonen, Taija Saloniemi-Heinonen, Petra Sipilä, Leena Strauss, Mahesh Tambe, Ashutosh Trehan, Heikki Turunen, Helena Virtanen and Fuping Zhang.

During these years I have been lucky to share the office with so many wonderful people. I wish to thank my current officemates Milena Doroszko, Freja Hartman Heidi Kemiläinen, Tiina Lehtiniemi, and Henriette Undeutch, and not forgetting the all past members of the B607, Ida Björkgren, Marcin Chrusciel, Matteo Da Ros, Hanna Korhonen, Oliver Meikar, Jenni Mäki-Jouppila, Emmi Rotgers, and Karin Sõstar and all the students who has made the B607 such a creative place to work. All students at the Department of Physiology Sheyla Cisneros Montalvo, Michael Gabriel, Janne Hakkarainen, Hanna Heikelä, Henna Henriksson, Riikka Huhtaniemi, Heli Jokela, Päivi Järvensivu, Matias Knuuttila, Jaakko

Koskenniemi, Gabriela Martínez Chacón, Opeyemi Olotu, Valeriy Paramonov, Konrad Patyra, Sofia Pruikkonen, Wiwat Rodpraset, Sergey Sadov, Ram Prakash Yadav, Anu Salminen, Anna Eggert, Meeri Jännäri, Titta Kivikoski, Emma Kutvonen, Tiina Lahtela, Lili Niinimäki, and Suvi Virtanen are acknowledged for their help and discussion during this thesis.

Work in the lab, day after day, would not have been possible without the help of excellent staff in the Department of Physiology. I especially want to thank Laboratory Manager Tuula Hämäläinen for creating functional working environment. My warmest gratitude goes to Johanna Järvi, Taina Kirjonen, Minna Lindroth, Marko Tirri, Pauliina Toivonen, Heidi Gerke, Katri Hovirinta, Anna Kostiander, Heidi Liljenbäck, Nina Messner, Mona Niiranen, Heli Niittymäki, Jonna Palmu, Pia Roering, Kati Asp, Marja-Riitta Kajaala, Erica Nyman, Taija Poikkipuoli, Minna Kangasperko, Leena Karlsson, Merja Leppiaho, Hannele Rekola, Anneli Vesa, and Eila Virransuo.

I wish to thank members from Animal genomics team; Daniel Fischer, Ilma Tapio, Miika Tapio, Maria Tuiskula-Haavisto and Johanna Vilkki. Terhi Iso-Touru is acknowledged of helping me to survive in the MTT/Luke and being the fastest sample shuttle between Turku and Jokioinen. I am very grateful for excellent technical staff; Tarja Hovivuori, Mervi Mutikainen, Johanna Rusi, Jonna Tabell, Anneli Virta, and Jouni Virta, who has been taking care of genotyping and various other lab works, that has lighten my workload tremendously.

Special thanks goes to Team Mänkuu. Without you girls, the journey through this thesis would have been even more painful. I wish to thank Heli, Marja and Hanna of all more or less “relaxing” moments that we have spent together. I also wish to thank Katri and Minna for their friendship, it means a lot to me.

Kiitos rakkaat vanhempani, Liisa ja Martti, että olette olleet aina tukenani ja auttaneet minua elämässä eteenpäin. Olette opettaneet minulle sitkeyttä, kärsivällisyyttä ja kunnianhimoa; elämäntaitoja, joita ilman tämänkin kirjan valmistuminen olisi ollut paljon vaikeampaa. Rakas isosiskoni Miia, Jari, A&O, kiitos mahtavista venereissuista, lastenhoitoavusta, remonttiavusta ja kaikesta läsnäolostanne matkan varrella. Kiitos Miia, teehetkistä ja sympatiasta, ne ovat olleet tärkeitä tälle tylsälle pikkusiskolle. Kiitos Pirkko ja Aatto, että olette aina tukeneet minua ja olleet läsnä arjessamme. Kiitos Helena ja Arto tuestanne ja lukuisista lastenhoitotunneista. Ne ovat tulleet todella tarpeeseen tämän projektin aikana.

I wish to thank my beloved husband, Miikkael, for your support, patience and your unconditional love. I appreciate so much all that hard work that you have

done at home to make our daily life better. This thesis would not have happened without your help. My precious little sunshine, Katariina, thank you for reminding me what the most important matters in life are.

The thesis work was financially supported by Academy of Finland, Turku Doctoral Programme on Molecular Medicine (TuDMM), Finnish Cultural Foundation, Häme and Varsinais-Suomi Regional funds, Turku University Foundation, University of Turku/Faculty of Medicine, Centre for Reproductive and Developmental Medicine and Oskar Öflunds Stiftelse.

Mari Lehti, Turku, November 2016

REFERENCES

Ahmed, E.A. & de Rooij, D.G. 2009, "Staging of mouse seminiferous tubule cross-sections", *Methods in molecular biology (Clifton, N.J.),* vol. 558, pp. 263-277.

Akhmanova, A., Mausset-Bonnefont, A.L., van Cappellen, W., Keijzer, N., Hoogenraad, C.C., Stepanova, T., Drabek, K., van der Wees, J., Mommaas, M., Onderwater, J., van der Meulen, H., Tanenbaum, M.E., Medema, R.H., Hoogerbrugge, J., Vreeburg, J., Uringa, E.J., Grootegoed, J.A., Grosveld, F. & Galjart, N. 2005, "The microtubule plus-end-tracking protein CLIP-170 associates with the spermatid manchette and is essential for spermatogenesis", *Genes & development,* vol. 19, no. 20, pp. 2501-2515.

Albee, A.J., Kwan, A.L., Lin, H., Granas, D., Stormo, G.D. & Dutcher, S.K. 2013, "Identification of cilia genes that affect cell-cycle progression using whole-genome transcriptome analysis in Chlamydomonas reinhardtti", *G3 (Bethesda, Md.),* vol. 3, no. 6, pp. 979-991.

Allan, V.J. 2011, "Cytoplasmic dynein", *Biochemical Society transactions,* vol. 39, no. 5, pp. 1169-1178.

Alves, M.M., Burzynski, G., Delalande, J., Osinga, J., van der Goot, A., Dolga, A.M., de Graaff, E., Brooks, A.S., Metzger, M., Eisel, U.L.M., Shepherd, I., Eggen, B.J.L. & Hofstra, R.M.W. 2010, "KBP interacts with SCG10, linking Goldberg–Shprintzen syndrome to microtubule dynamics and neuronal differentiation", *Human molecular genetics,* vol. 19, no. 18, pp. 3642-3651.

Andersson, M., Peltoniemi, O., Makinen, A., Sukura, A. & Rodriguez-Martinez, H. 2000, "The Hereditary ?Short Tail? Sperm Defect - A New Reproductive Problem in Yorkshire Boars", *Reproduction in Domestic Animals,* vol. 35, no. 2, pp. 59-63.

Antony, D., Becker-Heck, A., Zariwala, M.A., Schmidts, M., Onoufriadis, A., Forouhan, M., Wilson, R., Taylor-Cox, T., Dewar, A., Jackson, C., Goggin, P., Loges, N.T., Olbrich, H., Jaspers, M., Jorissen, M., Leigh, M.W., Wolf, W.E., Daniels, M.L., Noone, P.G., Ferkol, T.W., Sagel, S.D., Rosenfeld, M., Rutman, A., Dixit, A., O'Callaghan, C., Lucas, J.S., Hogg, C., Scambler, P.J., Emes, R.D., Uk10k, Chung, E.M., Shoemark, A., Knowles, M.R., Omran, H. & Mitchison, H.M. 2013, "Mutations in CCDC39 and CCDC40 are the major cause of primary ciliary dyskinesia with axonemal disorganization and absent inner dynein arms", *Human mutation,* vol. 34, no. 3, pp. 462-472.

Avasthi, P., Scheel, J.F., Ying, G., Frederick, J.M., Baehr, W. & Wolfrum, U. 2013, "Germline deletion of Cetn1 causes infertility in male mice", *Journal of cell science,* vol. 126, no. Pt 14, pp. 3204-3213.

Banu, Y., Matsuda, M., Yoshihara, M., Kondo, M., Sutou, S. & Matsukuma, S. 2002, "Golgi matrix protein gene, Golga3/Mea2, rearranged and re-expressed in pachytene spermatocytes restores spermatogenesis in the mouse", *Molecular reproduction and development,* vol. 61, no. 3, pp. 288-301.

Bellve, A.R., Cavicchia, J.C., Millette, C.F., O'Brien, D.A., Bhatnagar, Y.M. & Dym, M. 1977, "Spermatogenic cells of the prepuberal mouse. Isolation and morphological characterization", *The Journal of cell biology,* vol. 74, no. 1, pp. 68-85.

Bentson, L.F., Agbor, V.A., Agbor, L.N., Lopez, A.C., Nfonsam, L.E., Bornstein, S.S., Handel, M.A. & Linder, C.C. 2013, "New point mutation in Golga3 causes multiple defects in spermatogenesis", *Andrology,* vol. 1, no. 3, pp. 440-450.

Bhogaraju, S., Cajanek, L., Fort, C., Blisnick, T., Weber, K., Taschner, M., Mizuno, N., Lamla, S., Bastin, P., Nigg, E.A. & Lorentzen, E. 2013, "Molecular basis of tubulin transport within the cilium by IFT74 and IFT81", *Science (New York, N.Y.),* vol. 341, no. 6149, pp. 1009-1012.

Bhullar, B., Zhang, Y., Junco, A., Oko, R. & van der Hoorn, F.A. 2003, "Association of kinesin light chain with outer dense fibers in a microtubule-independent fashion", *The*

Journal of biological chemistry, vol. 278, no. 18, pp. 16159-16168.

Blanchon, S., Legendre, M., Copin, B., Duquesnoy, P., Montantin, G., Kott, E., Dastot, F., Jeanson, L., Cachanado, M., Rousseau, A., Papon, J.F., Beydon, N., Brouard, J., Crestani, B., Deschildre, A., Desir, J., Dollfus, H., Leheup, B., Tamalet, A., Thumerelle, C., Vojtek, A.M., Escalier, D., Coste, A., de Blic, J., Clement, A., Escudier, E. & Amselem, S. 2012, "Delineation of CCDC39/CCDC40 mutation spectrum and associated phenotypes in primary ciliary dyskinesia", *Journal of medical genetics,* vol. 49, no. 6, pp. 410-416.

Breitbart, H. 2002, "Intracellular calcium regulation in sperm capacitation and acrosomal reaction", *Molecular and cellular endocrinology,* vol. 187, no. 1–2, pp. 139-144.

Brown, P.R., Miki, K., Harper, D.B. & Eddy, E.M. 2003, "A-kinase anchoring protein 4 binding proteins in the fibrous sheath of the sperm flagellum", *Biology of reproduction,* vol. 68, no. 6, pp. 2241-2248.

Bunch, D.O., Welch, J.E., Magyar, P.L., Eddy, E.M. & O'Brien, D.A. 1998, "Glyceraldehyde 3-phosphate dehydrogenase-S protein distribution during mouse spermatogenesis", *Biology of reproduction,* vol. 58, no. 3, pp. 834-841.

Burfeind, P. & Hoyer-Fender, S. 1991, "Sequence and developmental expression of a mRNA encoding a putative protein of rat sperm outer dense fibers", *Developmental biology,* vol. 148, no. 1, pp. 195-204.

Calvi, A., Wong, A.S., Wright, G., Wong, E.S., Loo, T.H., Stewart, C.L. & Burke, B. 2015, "SUN4 is essential for nuclear remodeling during mammalian spermiogenesis", *Developmental biology,* vol. 407, no. 2, pp. 321-330.

Carbajal-Gonzalez, B.I., Heuser, T., Fu, X., Lin, J., Smith, B.W., Mitchell, D.R. & Nicastro, D. 2013, "Conserved structural motifs in the central pair complex of eukaryotic flagella", *Cytoskeleton (Hoboken, N.J.),* vol. 70, no. 2, pp. 101-120.

Carrera, A., Gerton, G.L. & Moss, S.B. 1994, "The major fibrous sheath polypeptide of mouse sperm: structural and functional similarities to the A-kinase anchoring proteins", *Developmental biology,* vol. 165, no. 1, pp. 272-284.

Chan, S.W., Fowler, K.J., Choo, K.H. & Kalitsis, P. 2005, "Spef1, a conserved novel testis protein found in mouse sperm flagella", *Gene,* vol. 353, no. 2, pp. 189-199.

Chuma, S., Hosokawa, M., Tanaka, T. & Nakatsuji, N. 2009, "Ultrastructural characterization of spermatogenesis and its evolutionary conservation in the germline: germinal granules in mammals", *Molecular and cellular endocrinology,* vol. 306, no. 1-2, pp. 17-23.

Crisp, M., Liu, Q., Roux, K., Rattner, J.B., Shanahan, C., Burke, B., Stahl, P.D. & Hodzic, D. 2006, "Coupling of the nucleus and cytoplasm: role of the LINC complex", *The Journal of cell biology,* vol. 172, no. 1, pp. 41-53.

Davenport, J.R., Watts, A.J., Roper, V.C., Croyle, M.J., van Groen, T., Wyss, J.M., Nagy, T.R., Kesterson, R.A. & Yoder, B.K. 2007, "Disruption of Intraflagellar Transport in Adult Mice Leads to Obesity and Slow-Onset Cystic Kidney Disease", *Current Biology,* vol. 17, no. 18, pp. 1586-1594.

Desgraz, R. & Herrera, P.L. 2009, "Pancreatic neurogenin 3-expressing cells are unipotent islet precursors", *Development (Cambridge, England),* vol. 136, no. 21, pp. 3567-3574.

Doiguchi, M., Mori, T., Toshimori, K., Shibata, Y. & Iida, H. 2002, "Spergen-1 might be an adhesive molecule associated with mitochondria in the middle piece of spermatozoa", *Developmental biology,* vol. 252, no. 1, pp. 127-137.

Dong, F., Shinohara, K., Botilde, Y., Nabeshima, R., Asai, Y., Fukumoto, A., Hasegawa, T., Matsuo, M., Takeda, H., Shiratori, H., Nakamura, T. & Hamada, H. 2014, "Pih1d3 is required for cytoplasmic preassembly of axonemal dynein in mouse sperm", *The Journal of cell biology,* vol. 204, no. 2, pp. 203-213.

Drevillon, L., Megarbane, A., Demeer, B., Matar, C., Benit, P., Briand-Suleau, A., Bodereau, V., Ghoumid, J., Nasser, M., Decrouy, X., Doco-Fenzy, M., Rustin, P., Gaillard, D., Goossens, M. & Giurgea, I. 2013, "KBP-cytoskeleton interactions underlie developmental anomalies in Goldberg-Shprintzen syndrome", *Human molecular genetics,* vol. 22, no. 12, pp. 2387-2399.

Dymek, E.E., Lefebvre, P.A. & Smith, E.F. 2004, "PF15p is the chlamydomonas homologue of the Katanin p80 subunit and is required for assembly of flagellar central microtubules", *Eukaryotic cell,* vol. 3, no. 4, pp. 870-879.

Eddy, E.M., Toshimori, K. & O'Brien, D.A. 2003, "Fibrous sheath of mammalian spermatozoa", *Microscopy research and technique,* vol. 61, no. 1, pp. 103-115.

Finn, R., Evans, C.C. & Lee, L. 2014, "Strain-dependent brain defects in mouse models of primary ciliary dyskinesia with mutations in Pcdp1 and Spef2", *Neuroscience,* vol. 277, pp. 552-567.

Fliegauf, M., Olbrich, H., Horvath, J., Wildhaber, J.H., Zariwala, M.A., Kennedy, M., Knowles, M.R. & Omran, H. 2005, "Mislocalization of DNAH5 and DNAH9 in respiratory cells from patients with primary ciliary dyskinesia", *American journal of respiratory and critical care medicine,* vol. 171, no. 12, pp. 1343-1349.

Follit, J.A., San Agustin, J.T., Xu, F., Jonassen, J.A., Samtani, R., Lo, C.W. & Pazour, G.J. 2008, "The Golgin GMAP210/TRIP11 anchors IFT20 to the Golgi complex", *PLoS genetics,* vol. 4, no. 12, pp. e1000315.

Follit, J.A., Tuft, R.A., Fogarty, K.E. & Pazour, G.J. 2006, "The intraflagellar transport protein IFT20 is associated with the Golgi complex and is required for cilia assembly", *Molecular biology of the cell,* vol. 17, no. 9, pp. 3781-3792.

Follit, J.A., Xu, F., Keady, B.T. & Pazour, G.J. 2009, "Characterization of mouse IFT complex B", *Cell motility and the cytoskeleton,* vol. 66, no. 8, pp. 457-468.

Franca, L.R., Hess, R.A., Dufour, J.M., Hofmann, M.C. & Griswold, M.D. 2016, "The Sertoli cell: one hundred fifty years of beauty and plasticity", *Andrology,* vol. 4, no. 2, pp. 189-212.

Frohnert, C., Schweizer, S. & Hoyer-Fender, S. 2011, "SPAG4L/SPAG4L-2 are testis-specific SUN domain proteins restricted to the apical nuclear envelope of round spermatids facing the acrosome", *Molecular human reproduction,* vol. 17, no. 4, pp. 207-218.

Fulcher, K.D., Mori, C., Welch, J.E., O'Brien, D.A., Klapper, D.G. & Eddy, E.M. 1995, "Characterization of Fsc1 cDNA for a mouse sperm fibrous sheath component", *Biology of reproduction,* vol. 52, no. 1, pp. 41-49.

Gob, E., Schmitt, J., Benavente, R. & Alsheimer, M. 2010, "Mammalian sperm head formation involves different polarization of two novel LINC complexes", *PloS one,* vol. 5, no. 8, pp. e12072.

Goduti, D.J. & Smith, E.F. 2012, "Analyses of functional domains within the PF6 protein of the central apparatus reveal a role for PF6 sub-complex members in regulating flagellar beat frequency", *Cytoskeleton,* vol. 69, no. 3, pp. 179-194.

Griswold, M.D. 1998, "The central role of Sertoli cells in spermatogenesis", *Seminars in cell & developmental biology,* vol. 9, no. 4, pp. 411-416.

Guan, J., Kinoshita, M. & Yuan, L. 2009, "Spatiotemporal association of DNAJB13 with the annulus during mouse sperm flagellum development", *BMC developmental biology,* vol. 9, pp. 23-213X-9-23.

Guichard, C., Harricane, M., Lafitte, J., Godard, P., Zaegel, M., Tack, V., Lalau, G. & Bouvagnet, P. 2001, "Axonemal Dynein Intermediate-Chain Gene (DNAI1) Mutations Result in Situs Inversus and Primary Ciliary Dyskinesia (Kartagener Syndrome)", *The American Journal of Human Genetics,* vol. 68, no. 4, pp. 1030-1035.

Hall, E.A., Keighren, M., Ford, M.J., Davey, T., Jarman, A.P., Smith, L.B., Jackson, I.J. & Mill, P. 2013, "Acute versus chronic loss of mammalian Azi1/Cep131 results in distinct ciliary phenotypes", *PLoS genetics,* vol. 9, no. 12, pp. e1003928.

Hall, E.S., Eveleth, J., Jiang, C., Redenbach, D.M. & Boekelheide, K. 1992, "Distribution of the microtubule-dependent motors cytoplasmic dynein and kinesin in rat testis", *Biology of reproduction,* vol. 46, no. 5, pp. 817-828.

Hermo, L., Pelletier, R.M., Cyr, D.G. & Smith, C.E. 2010a, "Surfing the wave, cycle, life history, and genes/proteins expressed by testicular germ cells. Part 1: background to spermatogenesis, spermatogonia, and spermatocytes", *Microscopy research and technique,* vol. 73, no. 4, pp. 241-278.

Hermo, L., Pelletier, R.M., Cyr, D.G. & Smith, C.E. 2010b, "Surfing the wave, cycle, life history, and genes/proteins expressed by testicular germ cells. Part 2: changes in spermatid organelles associated with development of spermatozoa", *Microscopy research and technique,* vol. 73, no. 4, pp. 279-319.

Hermo, L., Pelletier, R.M., Cyr, D.G. & Smith, C.E. 2010c, "Surfing the wave, cycle, life history, and genes/proteins expressed by testicular germ cells. Part 3: developmental changes in spermatid flagellum and cytoplasmic droplet and interaction of sperm with the zona pellucida and egg plasma membrane", *Microscopy research and technique,* vol. 73, no. 4, pp. 320-363.

Hess, R.A. & de Franca, L.R. 2008, "Spermatogenesis and Cycle of the Seminiferous Epithelium" in *Molecular Mechanisms in Spermatogenesis*, ed. C.Y. Cheng, Springer New York, , pp. 1-15.

Heuser, T., Raytchev, M., Krell, J., Porter, M.E. & Nicastro, D. 2009, "The dynein regulatory complex is the nexin link and a major regulatory node in cilia and flagella", *The Journal of cell biology,* vol. 187, no. 6, pp. 921-933.

Hicks, S.W., Horn, T.A., McCaffery, J.M., Zuckerman, D.M. & Machamer, C.E. 2006, "Golgin-160 promotes cell surface expression of the beta-1 adrenergic receptor", *Traffic (Copenhagen, Denmark),* vol. 7, no. 12, pp. 1666-1677.

Hicks, S.W. & Machamer, C.E. 2005, "Isoform-specific Interaction of Golgin-160 with the Golgi-associated Protein PIST", *Journal of Biological Chemistry,* vol. 280, no. 32, pp. 28944-28951.

Ho, H.C. & Wey, S. 2007, "Three dimensional rendering of the mitochondrial sheath morphogenesis during mouse spermiogenesis", *Microscopy research and technique,* vol. 70, no. 8, pp. 719-723.

Hogarth, C.A. & Griswold, M.D. 2010, "The key role of vitamin A in spermatogenesis", *The Journal of clinical investigation,* vol. 120, no. 4, pp. 956-962.

Hou, Y. & Witman, G.B. 2015, "Dynein and intraflagellar transport", *Experimental cell research,* vol. 334, no. 1, pp. 26-34.

Ihara, M., Kinoshita, A., Yamada, S., Tanaka, H., Tanigaki, A., Kitano, A., Goto, M., Okubo, K., Nishiyama, H., Ogawa, O., Takahashi, C., Itohara, S., Nishimune, Y., Noda, M. & Kinoshita, M. 2005, "Cortical organization by the septin cytoskeleton is essential for structural and mechanical integrity of mammalian spermatozoa", *Developmental cell,* vol. 8, no. 3, pp. 343-352.

Irons, M.J. & Clermont, Y. 1982, "Kinetics of fibrous sheath formation in the rat spermatid", *The American Journal of Anatomy,* vol. 165, no. 2, pp. 121-130.

Ito, C., Suzuki-Toyota, F., Maekawa, M., Toyama, Y., Yao, R., Noda, T. & Toshimori, K. 2004, "Failure to assemble the peri-nuclear structures in GOPC deficient spermatids as found in round-headed spermatozoa", *Archives of Histology and Cytology,* vol. 67, no. 4, pp. 349-360.

Jiang, L., Wei, Y., Ronquillo, C.C., Marc, R.E., Yoder, B.K., Frederick, J.M. & Baehr, W. 2015, "Heterotrimeric Kinesin-2 (KIF3) Mediates Transition Zone and Axoneme Formation of Mouse Photoreceptors",

Journal of Biological Chemistry, vol. 290, no. 20, pp. 12765-12778.

Johnson, K.A. & Rosenbaum, J.L. 1992, "Polarity of flagellar assembly in Chlamydomonas.", *The Journal of cell biology,* vol. 119, no. 6, pp. 1605-1611.

Johnson, K.J., Hall, E.S. & Boekelheide, K. 1996, "Kinesin localizes to the trans-Golgi network regardless of microtubule organization", *European journal of cell biology,* vol. 69, no. 3, pp. 276-287.

Johnson, L.R., Foster, J.A., Haig-Ladewig, L., VanScoy, H., Rubin, C.S., Moss, S.B. & Gerton, G.L. 1997, "Assembly of AKAP82, a protein kinase A anchor protein, into the fibrous sheath of mouse sperm", *Developmental biology,* vol. 192, no. 2, pp. 340-350.

Kang-Decker, N., Mantchev, G.T., Juneja, S.C., McNiven, M.A. & van Deursen, J.M. 2001, "Lack of acrosome formation in Hrb-deficient mice", *Science (New York, N.Y.),* vol. 294, no. 5546, pp. 1531-1533.

Kierszenbaum, A.L. 2002a, "Intramanchette transport (IMT): managing the making of the spermatid head, centrosome, and tail", *Molecular reproduction and development,* vol. 63, no. 1, pp. 1-4.

Kierszenbaum, A.L. 2002b, "Keratins: unraveling the coordinated construction of scaffolds in spermatogenic cells", *Molecular reproduction and development,* vol. 61, no. 1, pp. 1-2.

Kierszenbaum, A.L., Rivkin, E. & Tres, L.L. 2011, "Cytoskeletal track selection during cargo transport in spermatids is relevant to male fertility", *Spermatogenesis,* vol. 1, no. 3, pp. 221-230.

Kierszenbaum, A.L., Rivkin, E. & Tres, L.L. 2003a, "Acroplaxome, an F-actin-keratin-containing plate, anchors the acrosome to the nucleus during shaping of the spermatid head", *Molecular biology of the cell,* vol. 14, no. 11, pp. 4628-4640.

Kierszenbaum, A.L., Rivkin, E. & Tres, L.L. 2003b, "The actin-based motor myosin Va is a component of the acroplaxome, an acrosome-nuclear envelope junctional plate, and of manchette-associated vesicles", *Cytogenetic and genome research,* vol. 103, no. 3-4, pp. 337-344.

Kierszenbaum, A.L., Rivkin, E., Tres, L.L., Yoder, B.K., Haycraft, C.J., Bornens, M. & Rios, R.M. 2011, "GMAP210 and IFT88 are present in the spermatid golgi apparatus and participate in the development of the acrosome-acroplaxome complex, head-tail coupling apparatus and tail", *Developmental dynamics : an official publication of the American Association of Anatomists,* vol. 240, no. 3, pp. 723-736.

Kierszenbaum, A.L., Tres, L.L., Rivkin, E., Kang-Decker, N. & van Deursen, J.M. 2004, "The acroplaxome is the docking site of Golgi-derived myosin Va/Rab27a/b-containing proacrosomal vesicles in wild-type and Hrb mutant mouse spermatids", *Biology of reproduction,* vol. 70, no. 5, pp. 1400-1410.

Kissel, H., Georgescu, M.M., Larisch, S., Manova, K., Hunnicutt, G.R. & Steller, H. 2005, "The Sept4 septin locus is required for sperm terminal differentiation in mice", *Developmental cell,* vol. 8, no. 3, pp. 353-364.

Kondo, S., Sato-Yoshitake, R., Noda, Y., Aizawa, H., Nakata, T., Matsuura, Y. & Hirokawa, N. 1994, "KIF3A is a new microtubule-based anterograde motor in the nerve axon.", *The Journal of cell biology,* vol. 125, no. 5, pp. 1095-1107.

Korhonen, H.M., Meikar, O., Yadav, R.P., Papaioannou, M.D., Romero, Y., Da Ros, M., Herrera, P.L., Toppari, J., Nef, S. & Kotaja, N. 2011, "Dicer is required for haploid male germ cell differentiation in mice", *PloS one,* vol. 6, no. 9, pp. e24821.

Kotaja, N., Kimmins, S., Brancorsini, S., Hentsch, D., Vonesch, J.L., Davidson, I., Parvinen, M. & Sassone-Corsi, P. 2004, "Preparation, isolation and characterization of stage-specific spermatogenic cells for cellular and molecular analysis", *Nature methods,* vol. 1, no. 3, pp. 249-254.

Kotaja, N. & Sassone-Corsi, P. 2007, "The chromatoid body: a germ-cell-specific RNA-

processing centre", *Nature reviews.Molecular cell biology,* vol. 8, no. 1, pp. 85-90.

Kott, E., Duquesnoy, P., Copin, B., Legendre, M., Dastot-Le Moal, F., Montantin, G., Jeanson, L., Tamalet, A., Papon, J.F., Siffroi, J.P., Rives, N., Mitchell, V., de Blic, J., Coste, A., Clement, A., Escalier, D., Toure, A., Escudier, E. & Amselem, S. 2012, "Loss-of-function mutations in LRRC6, a gene essential for proper axonemal assembly of inner and outer dynein arms, cause primary ciliary dyskinesia", *American Journal of Human Genetics,* vol. 91, no. 5, pp. 958-964.

Kwitny, S., Klaus, A.V. & Hunnicutt, G.R. 2010, "The annulus of the mouse sperm tail is required to establish a membrane diffusion barrier that is engaged during the late steps of spermiogenesis", *Biology of reproduction,* vol. 82, no. 4, pp. 669-678.

Lechtreck, K.F. 2015, "IFT-Cargo Interactions and Protein Transport in Cilia", *Trends in biochemical sciences,* vol. 40, no. 12, pp. 765-778.

Lechtreck, K.F., Delmotte, P., Robinson, M.L., Sanderson, M.J. & Witman, G.B. 2008, "Mutations in Hydin impair ciliary motility in mice", *The Journal of cell biology,* vol. 180, no. 3, pp. 633-643.

Lechtreck, K.F., Gould, T.J. & Witman, G.B. 2013, "Flagellar central pair assembly in Chlamydomonas reinhardtii", *Cilia,* vol. 2, no. 1, pp. 15-2530-2-15.

Lechtreck, K.F. & Witman, G.B. 2007, "Chlamydomonas reinhardtii hydin is a central pair protein required for flagellar motility", *The Journal of cell biology,* vol. 176, no. 4, pp. 473-482.

Lehti, M.S. & Sironen, A. 2016, "Formation and function of manchette and flagellum during spermatogenesis", *Reproduction (Cambridge, England),* .

Li, W., Tang, W., Teves, M.E., Zhang, Z., Zhang, L., Li, H., Archer, K.J., Peterson, D.L., Williams, D.C.,Jr, Strauss, J.F.,3rd & Zhang, Z. 2015, "A MEIG1/PACRG complex in the manchette is essential for building the sperm flagella", *Development (Cambridge, England),* vol. 142, no. 5, pp. 921-930.

Linck, R.W., Chemes, H. & Albertini, D.F. 2016, "The axoneme: the propulsive engine of spermatozoa and cilia and associated ciliopathies leading to infertility", *Journal of assisted reproduction and genetics,* vol. 33, no. 2, pp. 141-156.

Liu, Y., DeBoer, K., de Kretser, D.M., O'Donnell, L., O'Connor, A.E., Merriner, D.J., Okuda, H., Whittle, B., Jans, D.A., Efthymiadis, A., McLachlan, R.I., Ormandy, C.J., Goodnow, C.C., Jamsai, D. & O'Bryan, M.K. 2015, "LRGUK-1 is required for basal body and manchette function during spermatogenesis and male fertility", *PLoS genetics,* vol. 11, no. 3, pp. e1005090.

Lyons, D.A., Naylor, S.G., Mercurio, S., Dominguez, C. & Talbot, W.S. 2008, "KBP is essential for axonal structure, outgrowth and maintenance in zebrafish, providing insight into the cellular basis of Goldberg-Shprintzen syndrome", *Development (Cambridge, England),* vol. 135, no. 3, pp. 599-608.

Manandhar, G., Simerly, C., Salisbury, J.L. & Schatten, G. 1999, "Centriole and centrin degeneration during mouse spermiogenesis", *Cell motility and the cytoskeleton,* vol. 43, no. 2, pp. 137-144.

Marszalek, J.R. & Goldstein, L.S. 2000, "Understanding the functions of kinesin-II", *Biochimica et biophysica acta,* vol. 1496, no. 1, pp. 142-150.

Marszalek, J.R., Liu, X., Roberts, E.A., Chui, D., Marth, J.D., Williams, D.S. & Goldstein, L.S. 2000, "Genetic evidence for selective transport of opsin and arrestin by kinesin-II in mammalian photoreceptors", *Cell,* vol. 102, no. 2, pp. 175-187.

Marszalek, J.R., Ruiz-Lozano, P., Roberts, E., Chien, K.R. & Goldstein, L.S. 1999, "Situs inversus and embryonic ciliary morphogenesis defects in mouse mutants lacking the KIF3A subunit of kinesin-II", *Proceedings of the National Academy of Sciences of the United States of America,* vol. 96, no. 9, pp. 5043-5048.

Matsuoka, Y., Iguchi, N., Kitamura, K., Nishimura, H., Manabe, H., Miyagawa, Y., Koga, M., Matsumiya, K., Okuyama, A., Tanaka, H. & Nishimune, Y. 2004, "Cloning and characterization of a mouse spergen-1 localized in sperm mitochondria", *International journal of andrology,* vol. 27, no. 3, pp. 152-160.

McKinney, T.D. & Desjardins, C. 1973, "Postnatal development of the testis, fighting behavior, and fertility in house mice", *Biology of reproduction,* vol. 9, no. 3, pp. 279-294.

Mei, X., Singh, I.S., Erlichman, J. & Orr, G.A. 1997, "Cloning and characterization of a testis-specific, developmentally regulated A-kinase-anchoring protein (TAKAP-80) present on the fibrous sheath of rat sperm", *European journal of biochemistry / FEBS,* vol. 246, no. 2, pp. 425-432.

Meikar, O. & Kotaja, N. 2014, "Isolation of chromatoid bodies from mouse testis as a rich source of short RNAs", *Methods in molecular biology (Clifton, N.J.),* vol. 1173, pp. 11-25.

Meikar, O., Vagin, V.V., Chalmel, F., Sostar, K., Lardenois, A., Hammell, M., Jin, Y., Da Ros, M., Wasik, K.A., Toppari, J., Hannon, G.J. & Kotaja, N. 2014, "An atlas of chromatoid body components", *RNA (New York, N.Y.),* vol. 20, no. 4, pp. 483-495.

Meinhardt, A., Wilhelm, B. & Seitz, J. 1999, "Expression of mitochondrial marker proteins during spermatogenesis", *Human reproduction update,* vol. 5, no. 2, pp. 108-119.

Miki, K. & Eddy, E.M. 1999, "Single amino acids determine specificity of binding of protein kinase A regulatory subunits by protein kinase A anchoring proteins", *The Journal of biological chemistry,* vol. 274, no. 41, pp. 29057-29062.

Miki, K. & Eddy, E.M. 1998, "Identification of tethering domains for protein kinase A type Ialpha regulatory subunits on sperm fibrous sheath protein FSC1", *The Journal of biological chemistry,* vol. 273, no. 51, pp. 34384-34390.

Miki, K., Qu, W., Goulding, E.H., Willis, W.D., Bunch, D.O., Strader, L.F., Perreault, S.D., Eddy, E.M. & O'Brien, D.A. 2004, "Glyceraldehyde 3-phosphate dehydrogenase-S, a sperm-specific glycolytic enzyme, is required for sperm motility and male fertility", *Proceedings of the National Academy of Sciences of the United States of America,* vol. 101, no. 47, pp. 16501-16506.

Miki, K., Willis, W.D., Brown, P.R., Goulding, E.H., Fulcher, K.D. & Eddy, E.M. 2002, "Targeted disruption of the Akap4 gene causes defects in sperm flagellum and motility", *Developmental biology,* vol. 248, no. 2, pp. 331-342.

Miller, M.G., Mulholland, D.J. & Vogl, A.W. 1999, "Rat testis motor proteins associated with spermatid translocation (dynein) and spermatid flagella (kinesin-II)", *Biology of reproduction,* vol. 60, no. 4, pp. 1047-1056.

Mitchell, D.R. & Sale, W.S. 1999, "Characterization of a Chlamydomonas insertional mutant that disrupts flagellar central pair microtubule-associated structures", *The Journal of cell biology,* vol. 144, no. 2, pp. 293-304.

Mitchell, D.R. & Smith, B. 2009, "Chapter 13 - Analysis of the Central Pair Microtubule Complex in Chlamydomonas reinhardtii", *Methods in cell biology,* vol. 92, pp. 197-213.

Moreno, R.D., Palomino, J. & Schatten, G. 2006, "Assembly of spermatid acrosome depends on microtubule organization during mammalian spermiogenesis", *Developmental biology,* vol. 293, no. 1, pp. 218-227.

Moreno, R.D. & Schatten, G. 2000, "Microtubule configurations and post-translational alpha-tubulin modifications during mammalian spermatogenesis", *Cell motility and the cytoskeleton,* vol. 46, no. 4, pp. 235-246.

Morimoto, A., Shibuya, H., Zhu, X., Kim, J., Ishiguro, K., Han, M. & Watanabe, Y. 2012, "A conserved KASH domain protein associates with telomeres, SUN1, and

dynactin during mammalian meiosis", *The Journal of cell biology,* vol. 198, no. 2, pp. 165-172.

Naaby-Hansen, S., Mandal, A., Wolkowicz, M.J., Sen, B., Westbrook, V.A., Shetty, J., Coonrod, S.A., Klotz, K.L., Kim, Y., Bush, L.A., Flickinger, C.J. & Herr, J.C. 2002, "CABYR, a Novel Calcium-Binding Tyrosine Phosphorylation-Regulated Fibrous Sheath Protein Involved in Capacitation", *Developmental biology,* vol. 242, no. 2, pp. 236-254.

Nagarkatti-Gude, D.R., Jaimez, R., Henderson, S.C., Teves, M.E., Zhang, Z. & Strauss, J.F.,3rd 2011, "Spag16, an axonemal central apparatus gene, encodes a male germ cell nuclear speckle protein that regulates SPAG16 mRNA expression", *PloS one,* vol. 6, no. 5, pp. e20625.

Nozawa, Y.I., Yao, E., Gacayan, R., Xu, S.M. & Chuang, P.T. 2014, "Mammalian Fused is essential for sperm head shaping and periaxonemal structure formation during spermatogenesis", *Developmental biology,* vol. 388, no. 2, pp. 170-180.

O'Donnell, L. & O'Bryan, M.K. 2014, "Microtubules and spermatogenesis", *Seminars in cell & developmental biology,* vol. 30, pp. 45-54.

O'Donnell, L., Rhodes, D., Smith, S.J., Merriner, D.J., Clark, B.J., Borg, C., Whittle, B., O'Connor, A.E., Smith, L.B., McNally, F.J., de Kretser, D.M., Goodnow, C.C., Ormandy, C.J., Jamsai, D. & O'Bryan, M.K. 2012, "An essential role for katanin p80 and microtubule severing in male gamete production", *PLoS genetics,* vol. 8, no. 5, pp. e1002698.

Olbrich, H., Schmidts, M., Werner, C., Onoufriadis, A., Loges, N.T., Raidt, J., Banki, N.F., Shoemark, A., Burgoyne, T., Al Turki, S., Hurles, M.E., UK10K Consortium, Kohler, G., Schroeder, J., Nurnberg, G., Nurnberg, P., Chung, E.M., Reinhardt, R., Marthin, J.K., Nielsen, K.G., Mitchison, H.M. & Omran, H. 2012, "Recessive HYDIN mutations cause primary ciliary dyskinesia without randomization of left-right body asymmetry", *American Journal of Human Genetics,* vol. 91, no. 4, pp. 672-684.

Olenick, M.A., Tokito, M., Boczkowska, M., Dominguez, R. & Holzbaur, E.L. 2016, "Hook Adaptors Induce Unidirectional Processive Motility by Enhancing the Dynein-Dynactin Interaction", *The Journal of biological chemistry,* vol. 291, no. 35, pp. 18239-18251.

Olson, G.E. & Sammons, D.W. 1980, "Structural chemistry of outer dense fibers of rat sperm", *Biology of reproduction,* vol. 22, no. 2, pp. 319-332.

Omran, H., Kobayashi, D., Olbrich, H., Tsukahara, T., Loges, N.T., Hagiwara, H., Zhang, Q., Leblond, G., O'Toole, E., Hara, C., Mizuno, H., Kawano, H., Fliegauf, M., Yagi, T., Koshida, S., Miyawaki, A., Zentgraf, H., Seithe, H., Reinhardt, R., Watanabe, Y., Kamiya, R., Mitchell, D.R. & Takeda, H. 2008, "Ktu/PF13 is required for cytoplasmic pre-assembly of axonemal dyneins", *Nature,* vol. 456, no. 7222, pp. 611-616.

Ostrowski, L.E., Andrews, K., Potdar, P., Matsuura, H., Jetten, A. & Nettesheim, P. 1999, "Cloning and characterization of KPL2, a novel gene induced during ciliogenesis of tracheal epithelial cells", *American journal of respiratory cell and molecular biology,* vol. 20, no. 4, pp. 675-683.

Parvinen, M. 2005, "The chromatoid body in spermatogenesis", *International journal of andrology,* vol. 28, no. 4, pp. 189-201.

Pasch, E., Link, J., Beck, C., Scheuerle, S. & Alsheimer, M. 2015, "The LINC complex component Sun4 plays a crucial role in sperm head formation and fertility", *Biology open,* vol. 4, no. 12, pp. 1792-1802.

Patel, V., Li, L., Cobo-Stark, P., Shao, X., Somlo, S., Lin, F. & Igarashi, P. 2008, "Acute kidney injury and aberrant planar cell polarity induce cyst formation in mice lacking renal cilia", *Human molecular genetics,* vol. 17, no. 11, pp. 1578-1590.

Petersen, C., Aumuller, G., Bahrami, M. & Hoyer-Fender, S. 2002, "Molecular cloning

of Odf3 encoding a novel coiled-coil protein of sperm tail outer dense fibers", *Molecular reproduction and development,* vol. 61, no. 1, pp. 102-112.

Phillips, D.M. 1980, "Observations on mammalian spermiogenesis using surface replicas", *Journal of ultrastructure research,* vol. 72, no. 1, pp. 103-111.

Praveen, K., Davis, E.E. & Katsanis, N. 2015, "Unique among ciliopathies: primary ciliary dyskinesia, a motile cilia disorder", *F1000prime reports,* vol. 7, pp. 36-36. eCollection 2015.

Roux, K.J., Crisp, M.L., Liu, Q., Kim, D., Kozlov, S., Stewart, C.L. & Burke, B. 2009, "Nesprin 4 is an outer nuclear membrane protein that can induce kinesin-mediated cell polarization", *Proceedings of the National Academy of Sciences,* vol. 106, no. 7, pp. 2194-2199.

Russell, L.D., Ettlin, R.A., SinhaHikim, A.P. & Clegg, E.D. 1990, *Histological and Histopathological EVALUATION OF THE TESTIS,* 1st edn, Cache River Press, United States.

Russell, L.D., Russell, J.A., MacGregor, G.R. & Meistrich, M.L. 1991, "Linkage of manchette microtubules to the nuclear envelope and observations of the role of the manchette in nuclear shaping during spermiogenesis in rodents", *The American Journal of Anatomy,* vol. 192, no. 2, pp. 97-120.

Samplaski, M.K., Agarwal, A., Sharma, R. & Sabanegh, E. 2010, "New generation of diagnostic tests for infertility: Review of specialized semen tests", *International Journal of Urology,* vol. 17, no. 10, pp. 839-847.

San Agustin, J.T., Pazour, G.J. & Witman, G.B. 2015, "Intraflagellar transport is essential for mammalian spermiogenesis but is absent in mature sperm", *Molecular biology of the cell,* vol. 26, no. 24, pp. 4358-4372.

Sapiro, R., Kostetskii, I., Olds-Clarke, P., Gerton, G.L., Radice, G.L. & Strauss III, J.F. 2002, "Male infertility, impaired sperm motility, and hydrocephalus in mice deficient in sperm-associated antigen 6", *Molecular and cellular biology,* vol. 22, no. 17, pp. 6298-6305.

Sapiro, R., Tarantino, L.M., Velazquez, F., Kiriakidou, M., Hecht, N.B., Bucan, M. & Strauss, J.F. 2000, "Sperm Antigen 6 Is the Murine Homologue of the Chlamydomonas reinhardtii Central Apparatus Protein Encoded by the PF16 Locus", *Biology of reproduction,* vol. 62, no. 3, pp. 511-518.

Saxena, D.K., Oh-Oka, T., Kadomatsu, K., Muramatsu, T. & Toshimori, K. 2002, "Behaviour of a sperm surface transmembrane glycoprotein basigin during epididymal maturation and its role in fertilization in mice", *Reproduction (Cambridge, England),* vol. 123, no. 3, pp. 435-444.

Schalles, U., Shao, X., van der Hoorn, F.A. & Oko, R. 1998, "Developmental expression of the 84-kDa ODF sperm protein: localization to both the cortex and medulla of outer dense fibers and to the connecting piece", *Developmental biology,* vol. 199, no. 2, pp. 250-260.

Shang, P., Baarends, W.M., Hoogerbrugge, J., Ooms, M.P., van Cappellen, W.A., de Jong, A.A., Dohle, G.R., van Eenennaam, H., Gossen, J.A. & Grootegoed, J.A. 2010, "Functional transformation of the chromatoid body in mouse spermatids requires testis-specific serine/threonine kinases", *Journal of cell science,* vol. 123, no. Pt 3, pp. 331-339.

Shao, X., Tarnasky, H.A., Lee, J.P., Oko, R. & van der Hoorn, F.A. 1999, "Spag4, a novel sperm protein, binds outer dense-fiber protein Odf1 and localizes to microtubules of manchette and axoneme", *Developmental biology,* vol. 211, no. 1, pp. 109-123.

Shao, X., Tarnasky, H.A., Schalles, U., Oko, R. & van der Hoorn, F.A. 1997, "Interactional cloning of the 84-kDa major outer dense fiber protein Odf84. Leucine zippers mediate associations of Odf84 and Odf27", *The Journal of biological chemistry,* vol. 272, no. 10, pp. 6105-6113.

Shao, X., Xue, J. & van der Hoorn, F.A. 2001, "Testicular protein Spag5 has similarity to mitotic spindle protein Deepest and binds outer dense fiber protein Odf1", *Molecular reproduction and development,* vol. 59, no. 4, pp. 410-416.

Sironen, A. 2009, *Molecular genetics of the immotile short tail sperm defect*, University of Turku.

Sironen, A., Hansen, J., Thomsen, B., Andersson, M., Vilkki, J., Toppari, J. & Kotaja, N. 2010, "Expression of SPEF2 during mouse spermatogenesis and identification of IFT20 as an interacting protein", *Biology of reproduction,* vol. 82, no. 3, pp. 580-590.

Sironen, A., Kotaja, N., Mulhern, H., Wyatt, T.A., Sisson, J.H., Pavlik, J.A., Miiluniemi, M., Fleming, M.D. & Lee, L. 2011, "Loss of SPEF2 function in mice results in spermatogenesis defects and primary ciliary dyskinesia", *Biology of reproduction,* vol. 85, no. 4, pp. 690-701.

Sironen, A., Thomsen, B., Andersson, M., Ahola, V. & Vilkki, J. 2006, "An intronic insertion in KPL2 results in aberrant splicing and causes the immotile short-tail sperm defect in the pig", *Proceedings of the National Academy of Sciences of the United States of America,* vol. 103, no. 13, pp. 5006-5011.

Sironen, A., Vilkki, J., Bendixen, C. & Thomsen, B. 2007, "Infertile Finnish Yorkshire boars carry a full-length LINE-1 retrotransposon within the KPL2 gene", *Molecular genetics and genomics : MGG,* vol. 278, no. 4, pp. 385-391.

Sironen, A.I., Andersson, M., Uimari, P. & Vilkki, J. 2002, "Mapping of an immotile short tail sperm defect in the Finnish Yorkshire on porcine Chromosome 16", *Mammalian genome : official journal of the International Mammalian Genome Society,* vol. 13, no. 1, pp. 45-49.

Smith, E.F. & Lefebvre, P.A. 1997, "PF20 gene product contains WD repeats and localizes to the intermicrotubule bridges in Chlamydomonas flagella.", *Molecular biology of the cell,* vol. 8, no. 3, pp. 455-467.

Smith, E.F. & Lefebvre, P.A. 1996, "PF16 encodes a protein with armadillo repeats and localizes to a single microtubule of the central apparatus in Chlamydomonas flagella", *The Journal of cell biology,* vol. 132, no. 3, pp. 359-370.

Steels, J.D., Estey, M.P., Froese, C.D., Reynaud, D., Pace-Asciak, C. & Trimble, W.S. 2007, "Sept12 is a component of the mammalian sperm tail annulus", *Cell motility and the cytoskeleton,* vol. 64, no. 10, pp. 794-807.

Sutton, K.A., Jungnickel, M.K., Wang, Y., Cullen, K., Lambert, S. & Florman, H.M. 2004, "Enkurin is a novel calmodulin and TRPC channel binding protein in sperm", *Developmental biology,* vol. 274, no. 2, pp. 426-435.

Teixido-Travesa, N., Roig, J. & Luders, J. 2012, "The where, when and how of microtubule nucleation - one ring to rule them all", *Journal of cell science,* vol. 125, no. Pt 19, pp. 4445-4456.

Teves, M.E., Jha, K.N., Song, J., Nagarkatti-Gude, D.R., Herr, J.C., Foster, J.A., Strauss, J.F.,3rd & Zhang, Z. 2013a, "Germ cell-specific disruption of the Meig1 gene causes impaired spermiogenesis in mice", *Andrology,* vol. 1, no. 1, pp. 37-46.

Teves, M.E., Zhang, Z., Costanzo, R.M., Henderson, S.C., Corwin, F.D., Zweit, J., Sundaresan, G., Subler, M., Salloum, F.N., Rubin, B.K. & Strauss, J.F.,3rd 2013b, "Sperm-associated antigen-17 gene is essential for motile cilia function and neonatal survival", *American journal of respiratory cell and molecular biology,* vol. 48, no. 6, pp. 765-772.

Toshimori, K. & Ito, C. 2003, "Formation and organization of the mammalian sperm head", *Archives of Histology and Cytology,* vol. 66, no. 5, pp. 383-396.

Toyo-Oka, K., Sasaki, S., Yano, Y., Mori, D., Kobayashi, T., Toyoshima, Y.Y., Tokuoka, S.M., Ishii, S., Shimizu, T., Muramatsu, M., Hiraiwa, N., Yoshiki, A.,

Wynshaw-Boris, A. & Hirotsune, S. 2005, "Recruitment of katanin p60 by phosphorylated NDEL1, an LIS1 interacting protein, is essential for mitotic cell division and neuronal migration", *Human molecular genetics,* vol. 14, no. 21, pp. 3113-3128.

Trapnell, C., Roberts, A., Goff, L., Pertea, G., Kim, D., Kelley, D.R., Pimentel, H., Salzberg, S.L., Rinn, J.L. & Pachter, L. 2012, "Differential gene and transcript expression analysis of RNA-seq experiments with TopHat and Cufflinks", *Nature protocols,* vol. 7, no. 3, pp. 562-578.

Turner, R.M. 2006, "Moving to the beat: a review of mammalian sperm motility regulation", *Reproduction, fertility, and development,* vol. 18, no. 1-2, pp. 25-38.

Turner, R.M. 2003, "Tales from the tail: what do we really know about sperm motility?", *Journal of andrology,* vol. 24, no. 6, pp. 790-803.

Ursini, F., Heim, S., Kiess, M., Maiorino, M., Roveri, A., Wissing, J. & Flohe, L. 1999, "Dual function of the selenoprotein PHGPx during sperm maturation", *Science (New York, N.Y.),* vol. 285, no. 5432, pp. 1393-1396.

Vera, J.C., Brito, M., Zuvic, T. & Burzio, L.O. 1984, "Polypeptide composition of rat sperm outer dense fibers. A simple procedure to isolate the fibrillar complex", *The Journal of biological chemistry,* vol. 259, no. 9, pp. 5970-5977.

Visconti, P.E., Johnson, L.R., Oyaski, M., Fornés, M., Moss, S.B., Gerton, G.L. & Kopf, G.S. 1997, "Regulation, Localization, and Anchoring of Protein Kinase A Subunits during Mouse Sperm Capacitation", *Developmental biology,* vol. 192, no. 2, pp. 351-363.

Welch, J.E., Schatte, E.C., O'Brien, D.A. & Eddy, E.M. 1992, "Expression of a glyceraldehyde 3-phosphate dehydrogenase gene specific to mouse spermatogenic cells", *Biology of reproduction,* vol. 46, no. 5, pp. 869-878.

Wilhelmsen, K., Litjens, S.H.M., Kuikman, I., Tshimbalanga, N., Janssen, H., van den Bout, I., Raymond, K. & Sonnenberg, A. 2005, "Nesprin-3, a novel outer nuclear membrane protein, associates with the cytoskeletal linker protein plectin", *The Journal of cell biology,* vol. 171, no. 5, pp. 799-810.

Williams, D., Hicks, S.W., Machamer, C.E. & Pessin, J.E. 2006, "Golgin-160 is required for the Golgi membrane sorting of the insulin-responsive glucose transporter GLUT4 in adipocytes", *Molecular biology of the cell,* vol. 17, no. 12, pp. 5346-5355.

Wilson, C.W., Nguyen, C.T., Chen, M.H., Yang, J.H., Gacayan, R., Huang, J., Chen, J.N. & Chuang, P.T. 2009, "Fused has evolved divergent roles in vertebrate Hedgehog signalling and motile ciliogenesis", *Nature,* vol. 459, no. 7243, pp. 98-102.

Wozniak, M.J., Melzer, M., Dorner, C., Haring, H.U. & Lammers, R. 2005, "The novel protein KBP regulates mitochondria localization by interaction with a kinesin-like protein", *BMC cell biology,* vol. 6, pp. 35.

Yadav, S., Puthenveedu, M.A. & Linstedt, A.D. 2012, "Golgin160 recruits the dynein motor to position the Golgi apparatus", *Developmental cell,* vol. 23, no. 1, pp. 153-165.

Yamazaki, H., Nakata, T., Okada, Y. & Hirokawa, N. 1996, "Cloning and characterization of KAP3: a novel kinesin superfamily-associated protein of KIF3A/3B", *Proceedings of the National Academy of Sciences of the United States of America,* vol. 93, no. 16, pp. 8443-8448.

Yamazaki, H., Nakata, T., Okada, Y. & Hirokawa, N. 1995, "KIF3A/B: a heterodimeric kinesin superfamily protein that works as a microtubule plus end-directed motor for membrane organelle transport", *The Journal of cell biology,* vol. 130, no. 6, pp. 1387-1399.

Yang, Z. & Goldstein, L.S.B. 1998, "Characterization of the KIF3C Neural Kinesin-like Motor from Mouse", *Molecular biology of the cell,* vol. 9, no. 2, pp. 249-261.

Yao, R., Ito, C., Natsume, Y., Sugitani, Y., Yamanaka, H., Kuretake, S., Yanagida, K., Sato, A., Toshimori, K. & Noda, T. 2002, "Lack of acrosome formation in mice lacking a Golgi protein, GOPC", *Proceedings of the National Academy of Sciences of the United States of America,* vol. 99, no. 17, pp. 11211-11216.

Yoshida, T., Ioshii, S.O., Imanaka-Yoshida, K. & Izutsu, K. 1994, "Association of cytoplasmic dynein with manchette microtubules and spermatid nuclear envelope during spermiogenesis in rats", *Journal of cell science,* vol. 107 (Pt 3), no. Pt 3, pp. 625-633.

Yuan, S., Stratton, C.J., Bao, J., Zheng, H., Bhetwal, B.P., Yanagimachi, R. & Yan, W. 2015, "Spata6 is required for normal assembly of the sperm connecting piece and tight head-tail conjunction", *Proceedings of the National Academy of Sciences of the United States of America,* vol. 112, no. 5, pp. E430-9.

Zhang, H. & Mitchell, D.R. 2004, "Cpc1, a Chlamydomonas central pair protein with an adenylate kinase domain", *Journal of cell science,* vol. 117, no. Pt 18, pp. 4179-4188.

Zhang, Q., Skepper, J.N., Yang, F., Davies, J.D., Hegyi, L., Roberts, R.G., Weissberg, P.L., Ellis, J.A. & Shanahan, C.M. 2001, "Nesprins: a novel family of spectrin-repeat-containing proteins that localize to the nuclear membrane in multiple tissues", *Journal of cell science,* vol. 114, no. Pt 24, pp. 4485-4498.

Zhang, Q., Ragnauth, C., Greener, M.J., Shanahan, C.M. & Roberts, R.G. 2002, "The Nesprins Are Giant Actin-Binding Proteins, Orthologous to Drosophila melanogaster Muscle Protein MSP-300", *Genomics,* vol. 80, no. 5, pp. 473-481.

Zhang, Y., Oko, R. & van der Hoorn, F.A. 2004, "Rat kinesin light chain 3 associates with spermatid mitochondria", *Developmental biology,* vol. 275, no. 1, pp. 23-33.

Zhang, Y., Ou, Y., Cheng, M., Shojaei Saadi, H., Thundathil, J.C. & van der Hoorn, F.A. 2012, "KLC3 is involved in sperm tail midpiece formation and sperm function", *Developmental biology,* vol. 366, no. 2, pp. 101-110.

Zhang, Z., Shen, X., Gude, D.R., Wilkinson, B.M., Justice, M.J., Flickinger, C.J., Herr, J.C., Eddy, E.M. & Strauss, J.F.,3rd 2009, "MEIG1 is essential for spermiogenesis in mice", *Proceedings of the National Academy of Sciences of the United States of America,* vol. 106, no. 40, pp. 17055-17060.

Zhang, Z., Kostetskii, I., Moss, S.B., Jones, B.H., Ho, C., Wang, H., Kishida, T., Gerton, G.L., Radice, G.L. & Strauss, J.F. 2004, "Haploinsufficiency for the murine orthologue of Chlamydomonas PF20 disrupts spermatogenesis", *Proceedings of the National Academy of Sciences of the United States of America,* vol. 101, no. 35, pp. 12946-12951.

Zhang, Z., Kostetskii, I., Tang, W., Haig-Ladewig, L., Sapiro, R., Wei, Z., Patel, A.M., Bennett, J., Gerton, G.L., Moss, S.B., Radice, G.L. & III, J.F.S. 2006, "Deficiency of SPAG16L Causes Male Infertility Associated with Impaired Sperm Motility", *Biology of reproduction,* vol. 74, no. 4, pp. 751-759.

Zhou, J., Yang, F., Leu, N.A. & Wang, P.J. 2012, "MNS1 is essential for spermiogenesis and motile ciliary functions in mice", *PLoS genetics,* vol. 8, no. 3, pp. e1002516.

Zuccarello, D., Ferlin, A., Cazzadore, C., Pepe, A., Garolla, A., Moretti, A., Cordeschi, G., Francavilla, S. & Foresta, C. 2008, "Mutations in dynein genes in patients affected by isolated non-syndromic asthenozoospermia", *Human Reproduction,* vol. 23, no. 8, pp. 1957-1962.